JOC*Article*

Excited-State Intramolecular Proton Transfer in 2-(2′-Arylsulfonamidophenyl)benzimidazole Derivatives: The Effect of Donor and Acceptor Substituents

Maged M. Henary, Yonggang Wu, John Cody, S. Sumalekshmy, Jing Li, Subrata Mandal, and Christoph J. Fahrni*

School of Chemistry and Biochemistry and Petit Institute for Bioengineering and Bioscience, Georgia Institute of Technology, 901 Atlantic Drive, Atlanta, Georgia 30332

fahrni@chemistry.gatech.edu

Received March 1, 2007

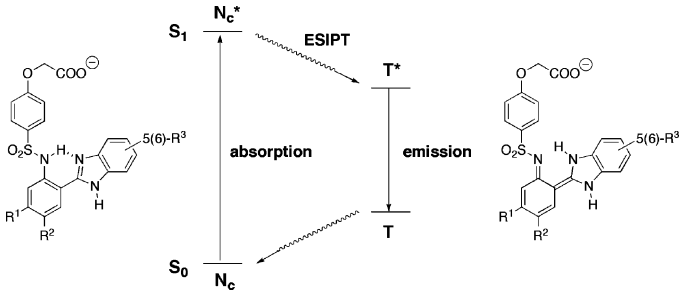

A series of water-soluble 2-(2′-arylsulfonamidophenyl)benzimidazole derivatives containing electron-donating and accepting groups attached to various positions of the fluorophore π-system has been synthesized and characterized in aqueous solution at 0.1 M ionic strength. The measured pK_a's for deprotonation of the sulfonamide group of monosubstituted derivatives range between 6.75 and 9.33 and follow closely Hammett's free energy relationship. In neutral aqueous buffer, all compounds undergo efficient excited-state intramolecular proton transfer (ESIPT) to yield a strongly Stokes-shifted fluorescence emission from the phototautomer. Upon deprotonation of the sulfonamide nitrogen at high pH, ESIPT is interrupted to yield a new, blue-shifted emission band. The peak absorption and emission energies were strongly influenced by the nature of the substituents and their attachment positions on the fluorophore π-system. The fluorescence quantum yield of the ESIPT tautomers revealed a significant correlation with the observed Stokes shifts. The study provides valuable information regarding substituent effects on the photophysical properties of this class of ESIPT fluorophores in an aqueous environment and may offer guidelines for designing emission ratiometric pH or metal-cation sensors for biological applications.

Introduction

Excited-state intramolecular proton transfer (ESIPT) represents a fundamental photophysical process that occurs in a wide range of fluorophores containing an intramolecular hydrogen bond. Upon photoexcitation, the proton moves from the hydrogen-bonding donor site to a nearby acceptor, resulting in ultrafast formation of an excited-state tautomer. Because a significant amount of excited-state energy is dissipated in this process, the phototautomer fluoresces at lower energy with an unusually large Stokes shift. Due to their unusual photophysical properties, ESIPT fluorophores have been extensively investigated as potential laser dyes,[1,2] photostabilizers,[3,4] scintillators,[5,6] hydrogen-bonding[7,8] and membrane polarity probes,[9,10] and as

* To whom correspondence should be addressed. Phone: 404-385-1164. Fax: 404-894-2295.

(1) Sakai, K.; Tsuzuki, T.; Itoh, Y.; Ichikawa, M.; Taniguchi, Y. *Appl. Phys. Lett.* **2005**, *86*, 081103.
(2) Costela, A.; Amat, F.; Catalan, J.; Douhal, A.; Figuera, J. M.; Munoz, J. M.; Acuna, A. U. *Opt. Commun.* **1987**, *64*, 457−460.
(3) Catalan, J.; Fabero, F.; Claramunt, R. M.; Maria, M. D. S.; Focesfoces, M. D. C.; Cano, F. H.; Martinezripoll, M.; Elguero, J.; Sastre, R. *J. Am. Chem. Soc.* **1992**, *114*, 5039−5048.
(4) Weichmann, M.; Port, H.; Laermer, F.; Frey, W.; Elsaesser, T. *Chem. Phys. Lett.* **1990**, *165*, 28−34.
(5) Kauffman, J. M. *Radiat. Phys. Chem.* **1993**, *41*, 365−371.
(6) Martinez, M. L.; Cooper, W. C.; Chou, P. T. *Chem. Phys. Lett.* **1992**, *193*, 151−154.
(7) McLaughlin, C. K.; Lantero, D. R.; Manderville, R. A. *J. Phys. Chem. A* **2006**, *110*, 6224−6230.

10.1021/jo070433l CCC: $37.00
Published on Web 05/25/2007

sensors for anions[11,12] or metal cations.[13−19] Among the diverse fluorophore architectures known to undergo ESIPT, aryl-substituted benzazoles (**I**) have been particularly extensively studied (Chart 1);[20−26] however, most of the work has focused on characterization of the unsubstituted fluorophore platform. To explore the effect of electron-donating and withdrawing groups on the photophysical properties of this class of fluorophores, we synthesized a series of benzimidazole derivatives with the general structure **II** containing cyano, methoxy, dimethylamino, or thiazolyl substituents attached to various positions of the fluorophore π-system. While the photophysics of 2-hydroxyphenyl-substituted benzimidazoles **I** ($X^1 = O$, $X^2 = NH$) is often complicated due to the presence of ground-state rotamers that cannot undergo ESIPT, their sulfonamide counterparts **II** ($X^1 = NHSO_2R$, $X^2 = NH$) exhibit clean ESIPT emission with high quantum yield in a wide range of solvents.[14,27] For the present study, we therefore chose aryl-sulfonamides as hydrogen-bonding donors rather than phenols. Given our interest in the development of fluorescent sensors for biological applications, we characterized all compounds in aqueous solution at 0.1 M ionic background. To increase the solubility under these conditions, we functionalized the fluorophore with a carboxylic acid group that is expected to be fully dissociated at pH 6 or higher. Of particular interest was the question of to what extent the substituents might shift the UV−vis absorption and ESIPT fluorescence bands toward lower energy, a desirable property for minimizing background fluorescence in context of biological imaging applications. Furthermore, we were interested in the photophysical properties of the fully deprotonated fluorophore, which, due to the absence of the sulfonamide proton, cannot undergo ESIPT and should emit with normal Stokes shift at higher energy. This property of ESIPT fluorophores is a particularly attractive feature for the design of emission ratiometric pH or metal-cation sensors.[14,15,17,18]

CHART 1

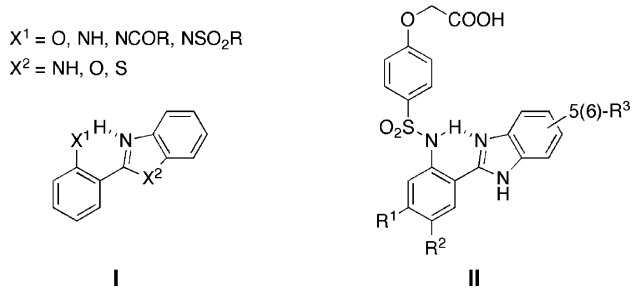

Results and Discussion

1. Synthesis. Scheme 1 outlines the two synthetic routes that were utilized for the synthesis of benzimidazole derivatives **5a**−**5l**. Key step in both routes is formation of the benzimidazole ring from the corresponding substituted aryl precursors. While the condensation of carboxylic acids with phenylenediamines provides facile access to 2-aryl-substituted benzimidazoles,[28] the reaction proceeds typically only under harsh conditions which are not compatible with functional groups such as carboxylic acid esters or nitriles. Alternatively, phenylenediamine can be condensed with aldehydes to give the corresponding imine intermediate, which is, upon ring-closing to the aminal, readily oxidized under mild conditions to yield the desired benzimidazoles.[14] We found that the latter strategy was well suited for the synthesis of the substituted benzimidazole derivatives **5a**−**5l**. Due to rapid annular tautomerization, derivatives **5c** and **5h**−**5k** with a substituent R^3 attached to the benzimidazole ring are obtained as mixtures of the corresponding 5- and 6-substituted tautomers (vide infra).

As outlined in Scheme 1, the aryl-sulfonamide moiety was installed either prior or after formation of the benzimidazole ring. In the latter case (route A), the amino functionality was first masked as a nitro group. After oxidative coupling with the corresponding phenylenediamine derivative, the nitro group in intermediates **2a**−**2e** was reduced to the amine by palladium-catalyzed hydrogenation at ambient pressure. These conditions were sufficiently mild such that the cyano group remained unaffected in the conversion of **2b** to **3b**. The synthesis was concluded by coupling of **3** with the sulfonyl chloride derivative[14] **10** followed by selective hydrolysis of the carboxylate ester to give the water-soluble fluorophores **5a**−**5e**.

Installation of the sulfonamide moiety prior to formation of the benzimidazole ring (route B) led through intermediates **9**, which served as versatile precursors for the synthesis of a range of substituted benzimidazoles **4f**−**4l**. The syntheses were again completed with hydrolysis of the carboxylate esters to give fluorophores **5f**−**5l**. Methoxy- and dimethylamino-substituted intermediates **9f** and **9g** were obtained from the corresponding nitro derivatives **1f** and **1g**, respectively, which, after reduction to the amine, were coupled with sulfonyl chloride **10**. The synthesis of both derivatives succeeded with moderate to low yields (45% and 28%, respectively), which is presumably due to the instability of intermediate **6** toward formation of oli-

(8) Shynkar, V. V.; Klymchenko, A. S.; Piemont, E.; Demchenko, A. P.; Mely, Y. *J. Phys. Chem. A* **2004**, *108*, 8151−8159.
(9) Klymchenko, A. S.; Duportail, G.; Mely, Y.; Demchenko, A. P. *Proc. Natl. Acad. Sci. U.S.A.* **2003**, *100*, 11219−11224.
(10) Klymchenko, A. S.; Duportail, G.; Ozturk, T.; Pivovarenko, V. G.; Mely, Y.; Demchenko, A. P. *Chem. Biol.* **2002**, *9*, 1199−1208.
(11) Klymchenko, A. S.; Demchenko, A. P. *J. Am. Chem. Soc.* **2002**, *124*, 12372−12379.
(12) Pivovarenko, V. G.; Vadzyuk, O. B.; Kosterin, S. O. *J. Fluoresc.* **2006**, *16*, 9−15.
(13) Henary, M. M.; Fahrni, C. J. *J. Phys. Chem. A* **2002**, *106*, 5210−5220.
(14) Henary, M. M.; Wu, Y.; Fahrni, C. J. *Chem. Eur. J.* **2004**, *10*, 3015−3025.
(15) Ohshima, A.; Momotake, A.; Arai, T. *Tetrahedron Lett.* **2004**, *45*, 9377−9381.
(16) Qin, W.; Obare, S. O.; Murphy, C. J.; Angel, S. M. *Analyst* **2001**, *126*, 1499−1501.
(17) Roshal, A. D.; Grigorovich, A. V.; Doroshenko, A. O.; Pivovarenko, V. G.; Demchenko, A. P. *J. Phys. Chem. A* **1998**, *102*, 5907−5914.
(18) Tanaka, K.; Kumagai, T.; Aoki, H.; Deguchi, M.; Iwata, S. *J. Org. Chem.* **2001**, *66*, 7328−7333.
(19) Zhang, X. B.; Peng, J.; He, C. L.; Shen, G. L.; Yu, R. Q. *Anal. Chim. Acta* **2006**, *567*, 189−195.
(20) Abou-Zied, O. K.; Jimenez, R.; Thompson, E. H. Z.; Millar, D. P.; Romesberg, F. E. *J. Phys. Chem. A* **2002**, *106*, 3665−3672.
(21) Barbara, P. F.; Brus, L. E.; Rentzepis, P. M. *J. Am. Chem. Soc.* **1980**, *102*, 5631−5635.
(22) Das, K.; Sarkar, N.; Majumdar, D.; Bhattacharyya, K. *Chem. Phys. Lett.* **1992**, *198*, 443−448.
(23) Douhal, A.; Amat-Guerri, F.; Lillo, M. P.; Acuna, A. U. *J. Photochem. Photobiol., A* **1994**, *78*, 127−138.
(24) Lochbrunner, S.; Wurzer, A. J.; Riedle, E. *J. Phys. Chem. A* **2003**, *107*, 10580−10590.
(25) Pla-Dalmau, A. *J. Org. Chem.* **1995**, *60*, 5468−5473.
(26) Roberts, E. L.; Dey, J.; Warner, I. M. *J. Phys. Chem. A* **1997**, *101*, 5296−5301.
(27) Fahrni, C. J.; Henary, M. M.; VanDerveer, D. G. *J. Phys. Chem. A* **2002**, *106*, 7655−7663.
(28) Phillips, M. A. *J. Chem. Soc.* **1928**, 2393−2399.

SCHEME 1

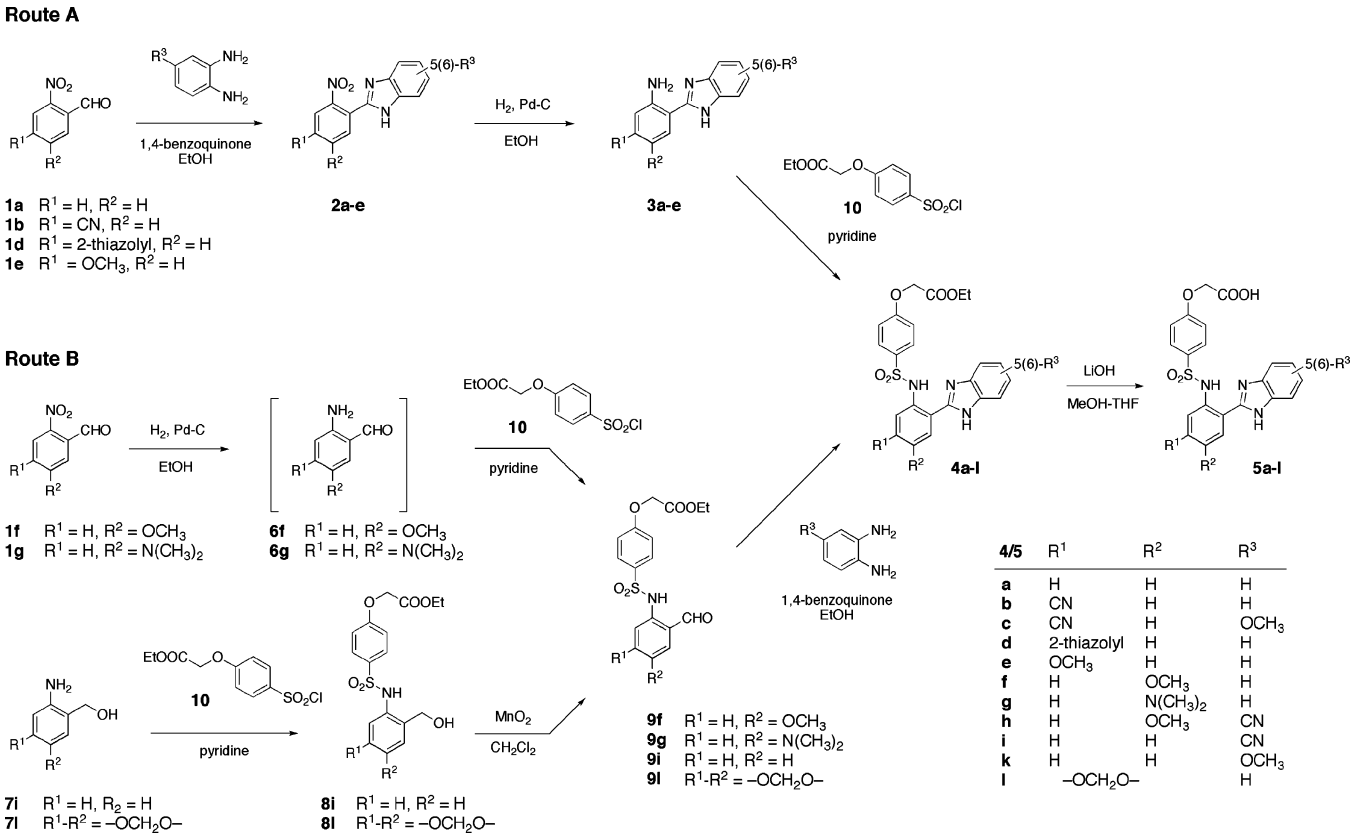

4/5	R^1	R^2	R^3
a	H	H	H
b	CN	H	H
c	CN	H	OCH_3
d	2-thiazolyl	H	H
e	OCH_3	H	H
f	H	OCH_3	H
g	H	$N(CH_3)_2$	H
h	H	OCH_3	CN
i	H	H	CN
k	H	H	OCH_3
l	$-OCH_2O-$		H

goimines. In the case of intermediates **9i** and **9l**, we thought to bypass this problem by starting with the corresponding aminobenzyl alcohols **7i** and **7l**, which were reacted with sulfonyl chloride **10** and then oxidized to give aldehydes **9i** and **9l**, respectively. However, the yield did not improve substantially and was even lower in the case of **9l**, thus rendering this pathway less attractive compared to the first approach.

Although in the present study the strategy for synthesizing a particular derivative was primarily governed by the accessibility of the starting materials, the two routes A and B outlined in Scheme 1 offer distinct synthetic flexibilities. Because the sulfonamide moiety is installed toward the end of route A, this approach is well suited for optimizing fluorophore properties that depend on the nature of the sulfonamide substituent, for example the pK_a of the sulfonamide nitrogen. In contrast, route B offers the opportunity to readily change the substituents on the benzimidazole ring, for example to tune the photophysical properties of the fluorophore or to build a multidentate ligand environment for optimizing the selectivity and affinity toward coordination of metal cations.[14]

2. Ground-State Protonation Equilibria. To study the substituent effects without being misled by pH-dependent absorption changes, it was necessary to determine the UV−vis and fluorescence emission spectra under conditions at which the sulfonamide group is either fully protonated or deprotonated. While spectra of the latter species (L^{2-}) are readily obtained at high pH, quantitative protonation of the sulfonamide nitrogen might require a proton concentration at which significant amounts of the double-protonated species (LH_2) are also present. To alleviate this problem, we determined the UV−vis spectra of the monoprotonated fluorophores LH^- from pH titrations by means of spectral deconvolution, which at the same time yielded the corresponding pK_a values for each protonation equilibrium. As exemplified by the titration of fluorophore **5f**, a set of UV−vis absorption spectra were acquired over the pH range of 4−10 at 0.1 M ionic strength (Figure 1a). The traces revealed two sets of isosbestic points suggesting two distinct protonation equilibria. Least-squares fit analysis over the entire spectral range provided deconvoluted absorption spectra along with the pK_a's for each of the two protonation equilibria. On basis of the large shifts in the absorption spectrum, the first pK_a of 8.34 can be unambiguously assigned to protonation of the sulfonamide nitrogen. In contrast, the second pK_a of 4.54 involved only small absorption changes, which are consistent with protonation of the electronically decoupled carboxylate group rather than the benzimidazole nitrogen. A species distribution diagram calculated from these data indicates (Figure 1b) that the monoprotonated fluorophore LH^- is present as a single species only within a rather narrow pH range centered around $-\log[H_3O^+] = 6.5$.

Following this approach, the pK_a values were measured for the protonation equilibria of each fluorophore (Table 1). To determine the $-\log[H_3O^+]$ value at which the monoprotonated species LH^- is most abundant, a species distribution diagram was calculated for each compound. The corresponding proton concentrations obtained from these analyses are compiled in Table 1. In addition, the last column in Table 1 indicates the calculated fractional concentration of fully deprotonated ligand that is present at that proton concentration. All fluorescence emission spectra and quantum yields of the monoprotonated species LH^- were acquired at this $-\log[H_3O^+]$ value without further deconvolution. All spectral data, including absorption and emission maxima, Stokes shifts, and fluorescence quantum yields, are listed in Table 2. For comparison, the data previously

TABLE 1. Protonation Constants of Benzimidazole Derivatives 5a−5l in Aqueous Solution[a]

	substituents						
	R_1	R_2	R_3	pK_{a1}[b]	pK_{a2}[c]	$-\log[H_3O^+]$[d]	$[L^{2-}]/[L]_{tot}$ [%][e]
5a[f]	H	H	H	8.04 ± 0.03	4.46 ± 0.08	7.0	4
5b	CN	H	H	6.75 ± 0.02	n.d.[g]	5.2	3
5c	CN	H	OCH_3	6.88 ± 0.03	n.d.[g]	5.2	3
5d	2-thiazolyl	H	H	7.30 ± 0.01	n.d.[g]	6.0	3
5e	OCH_3	H	H	7.60 ± 0.01	4.79 ± 0.03	6.2	3
5f	H	OCH_3	H	8.34 ± 0.01	4.53 ± 0.06	6.5	<1
5g	H	$N(CH_3)_2$	H	9.33 ± 0.05	8.01 ± 0.02[h]	6.7	<1
5h	H	OCH_3	CN	7.96 ± 0.02	5.51 ± 0.1	6.7	5
5i	H	H	CN	7.63 ± 0.02	5.21 ± 0.1	6.5	6
5k	H	H	OCH_3	7.95 ± 0.02	4.91 ± 0.1	6.5	3
5l	$-OCH_2O-$		H	7.98 ± 0.01	4.65 ± 0.02	6.3	1

[a] 0.1 M KCl, 25 °C. [b] $K_{a1} = [L^{2-}][H^+]/[LH^-]$. [c] $K_{a2} = [LH^-][H^+]/[LH_2]$. [d] Proton concentration used for photophysical characterization of LH^-. [e] Residual concentration of fully deprotonated L^{2-}. [f] Data from ref 14. [g] Spectral deconvolution insufficient for accurate determination. [h] Protonation of the carboxylate group occurs at $pK_{a3} = 4.81 \pm 0.05$.

TABLE 2. Photophysical Data of Benzimidazole Derivatives 5a−5l in Aqueous Solution[a]

	monoprotonated species (LH^-)				deprotonated species (L^{2-})					
	abs λ_{max} [nm][b]	em λ_{max} [nm][c]	Stokes shift [cm^{-1}]	Φ_F[c]	abs λ_{max} [nm][b]	em λ_{max} [nm][d]	Stokes shift [cm^{-1}]	Φ_F[d]	isosbestic point [nm]	emission shift [nm][e]
5a[f]	300	460	11 590	0.23	329	418	6470	0.26	315	42
5b	319	483 (404)	10 640	0.37	355	447	5800	0.70	341	36
5c	341	481	8540	0.46	362	452	5500	0.34	350	29
5d	331	484 (403)	9550	0.41	361	475	6650	0.42	352	9
5e	305	432	9640	0.17[g]	329	396	5140	0.06	314	36
5f	298	497	13 440	0.14	334	444	7420	0.27	322	53
5g	273	568 (448)	14 760[h]	<0.01	348	505	8930	0.08	296	63
5h	306	534	13 950	0.03	340	480	8580	0.02	326	54
5i	307	489	12 120	0.25	333	452	7910	0.29	320	37
5k	316	452	9520	0.13	333	416	5990	0.29	320	36
5l	314	459	10 060	0.04	340	423	5770	0.04	326	36

[a] 0.1 M KCl, 25 °C. [b] From deconvolution analysis. [c] At the proton concentration as indicated in Table 1; excitation at isosbestic point. [d] pH 10.8, 0.1 M KCl. [e] Difference of peak emission wavelength of species LH^- and L^{2-}. [f] Data from ref 14. [g] Excitation at 370 nm increases the quantum yield to 0.35. [h] Based on excitation spectrum acquired at 650 nm.

SCHEME 2

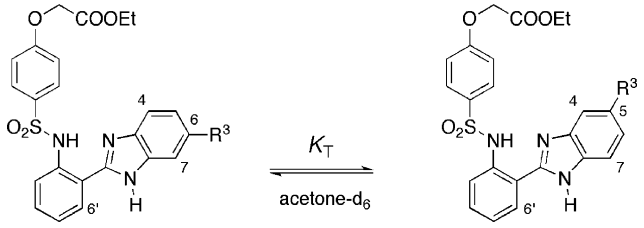

reported[14] for the unsubstituted parent fluorophore **5a** are also included in Tables 1 and 2.

The measured acidity constants for deprotonation of the sulfonamide nitrogen range between 6.7 and 9.3 and depend strongly on the nature and attachment position of the substituents (Table 1). The measured pK_a's follow closely Hammett's free energy relationship (Figure 2),[29] thus directly reflecting the degree of resonance stabilization and inductive effects imposed by the corresponding substituents. For example, substitution with a methoxy group in the para-position to the sulfonamide group increased the pK_a by 0.3 units (compound **5f**), while substitution in the meta-position resulted in a decrease by 0.4 units (compound **5e**). In the former case, resonance stabilization dominates over the inductive effect imposed by the electronegative oxygen, while in the latter case the opposite holds true. Substitution with a dimethylamino group, a stronger π-donor compared to methoxy, further increased the sulfonamide pK_a to 9.33 (compound **5g**). As expected, the electron-withdrawing cyano substituent significantly increased the acidity of the sulfonamide group. The effect is more pronounced if CN is attached to the central aryl ring (compound **5b**) than the benzimidazole moiety (compound **5i**). Consistent with the smaller electron-withdrawing ability of the 2-thiazolyl substituent, the sulfonamide in **5d** is less acidic than that in **5b** but still more acidic than that in the unsubstituted parent compound **5a**. The double-substituted compounds **5c** and **5h** exhibit pK_a's that reflect the influence of both groups; however, substitution on the central aryl ring appears to carry more weight compared to substitution on the benzimidazole ring.

3. Ground-State Tautomerism. In solution, 1*H*-benzimidazole derivatives are typically subject to rapid annular tautomerization.[14,31] Whereas the N1(H)/N3(H) prototropic equilibrium of unsubstituted benzimidazole is energetically degenerate, derivatives with a substituent R^3 attached to the benzimidazole ring yield a nondegenerate tautomer pair (Scheme 2). The concentration ratio of the two species at equilibrium corresponds to the tautomeric equilibrium constant K_T which can be used to estimate the stability difference $\Delta G_T = -RT\ln K_T$ of the tautomer pair.

(29) Hammett, L. P. *J. Am. Chem. Soc.* **1937**, *59*, 96−103.
(30) Hansch, C.; Leo, A.; Taft, R. W. *Chem. Rev.* **1991**, *91*, 165−195.
(31) Minkin, V. I.; Garnovskii, A. D.; Elguero, J.; Katritzky, A. R.; Denisko, O. V. In *Advances in Heterocyclic Chemistry*; Katritzky, A. R., Ed.; Academic Press: New York, 2000; Vol. 76, pp 157−323.

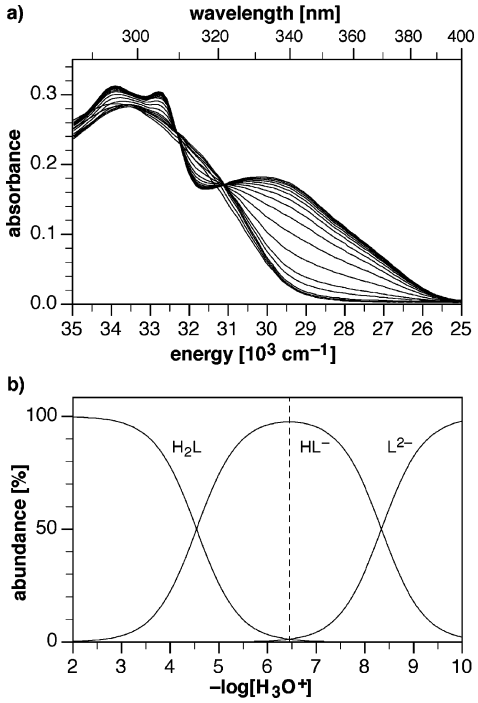

FIGURE 1. (a) Spectrophotometric pH titration of fluorophore **5f** in aqueous solution (0.1 M KCl, 25 °C). (b) Calculated species distribution diagram for fluorophore **5f**.

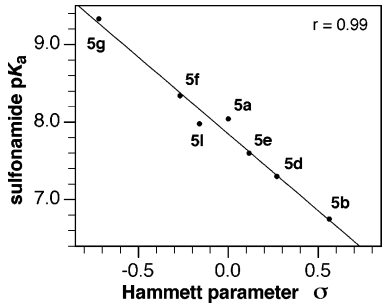

FIGURE 2. Linear dependence of the sulfonamide acidity (pK_{a1}) on Hammett's σ parameters (ref 30) for monosubstituted fluorophores **5a**, **5b**, **5d**−**5g**, and **5l** (r = correlation coefficient).

To investigate the effect of the 5(6)-cyano and 5(6)-methoxy substituents on the energetics of the tautomerization equilibrium, we performed a series of variable temperature ^{1}H NMR experiments with derivatives **4i** and **4k**. While the exchange kinetics in protic solvents lies at the fast exchange limit with regard to the NMR time scale,[14] the tautomerization proved to be sufficiently slow in acetone-d_6 at cryo temperatures. As illustrated in Figure 3, the ^{1}H NMR spectrum of cyano-substituted **4i** exhibited exchange-broadened benzimidazole proton resonances that gradually sharpened up with decreasing temperature. At −60 °C two sets of well-resolved signals were observed for the two tautomers, indicating slow exchange with regard to the NMR time scale. From the integrated intensity ratio of the C4(H) and C7(H) resonances at 8.43 and 8.11 ppm, a tautomeric equilibrium constant of $K_T = 1.43 \pm 0.008$ was measured, corresponding to a free energy difference of $\Delta G_T = 0.63 \pm 0.01$ kJ mol^{-1}.

To elucidate whether the equilibrium position is in favor of the 5- or 6-cyano-substituted tautomer of **4i**, we performed a 2D NOESY experiment at −80 °C in acetone-d_6 (Figure 4, left).

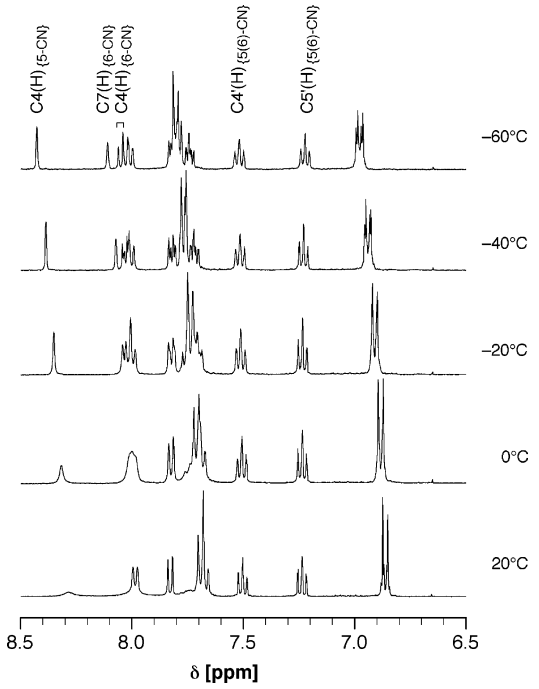

FIGURE 3. Variable temperature ^{1}H NMR spectra 5(6)-cyano-substituted benzimidazole derivative **4i** in acetone-d_6 (20 mM).

At this temperature, the exchange kinetics was sufficiently slow such that the tautomer pair yielded two well-separated benzimidazole NH resonances. As indicated by the dashed lines in Figure 4 (left), the NH proton at 13.40 ppm is in NOE contact with the benzimidazole proton C7(H) appearing as a singlet at 8.17 ppm, while the more intense, upfield-shifted NH proton at 13.32 ppm shows a correlation with the doublet resonance at 7.83 ppm. On the basis of these NOE contacts it is possible to unambiguously identify the 5-cyano-substituted tautomer as the major species, which, in concurrence with the experimental data, is expected to show an NOE correlation between N1(H)/C7(H) but not between N1(H)/C4(H). A quantum chemical study of 5(6)-cyano-benzimidazole at the AM1 level of theory predicted also the 5-substituted tautomer to be slightly more stable ($K_T = 1.62$) compared to its 6-substituted counterpart.[32] Accordingly, intramolecular hydrogen bonding with the neighboring sulfonamide proton does not appear to significantly alter the position of the tautomeric equilibrium of **4i**.

The corresponding low-temperature 2D NOESY NMR experiment of methoxy-substituted derivative **4k** revealed that the 6- rather than 5-substituted tautomer is the major species (Figure 4, right). The measured tautomerization equilibrium constant lies with $K_T = 0.66 \pm 0.01$ also near unity, corresponding to a similarly small free energy difference of $\Delta G_T = 0.66 \pm 0.01$ kJ mol^{-1} for the methoxy-substituted tautomer pair. In agreement with the computational study,[32] differences in tautomer stabilities seem to be primarily governed by substituent-dependent resonance effects, whereas polarizability and inductive contributions appear less important. In summary, given the rapid tautomerization kinetics combined with near unity equilibrium constants for the investigated 5(6)-substituted benzimidazole derivatives, the photophysical data must be interpreted as averaged properties of the two tautomers.

(32) Raczynska, E. D. *J. Chem. Res., Synop.* **1998**, 704−705.

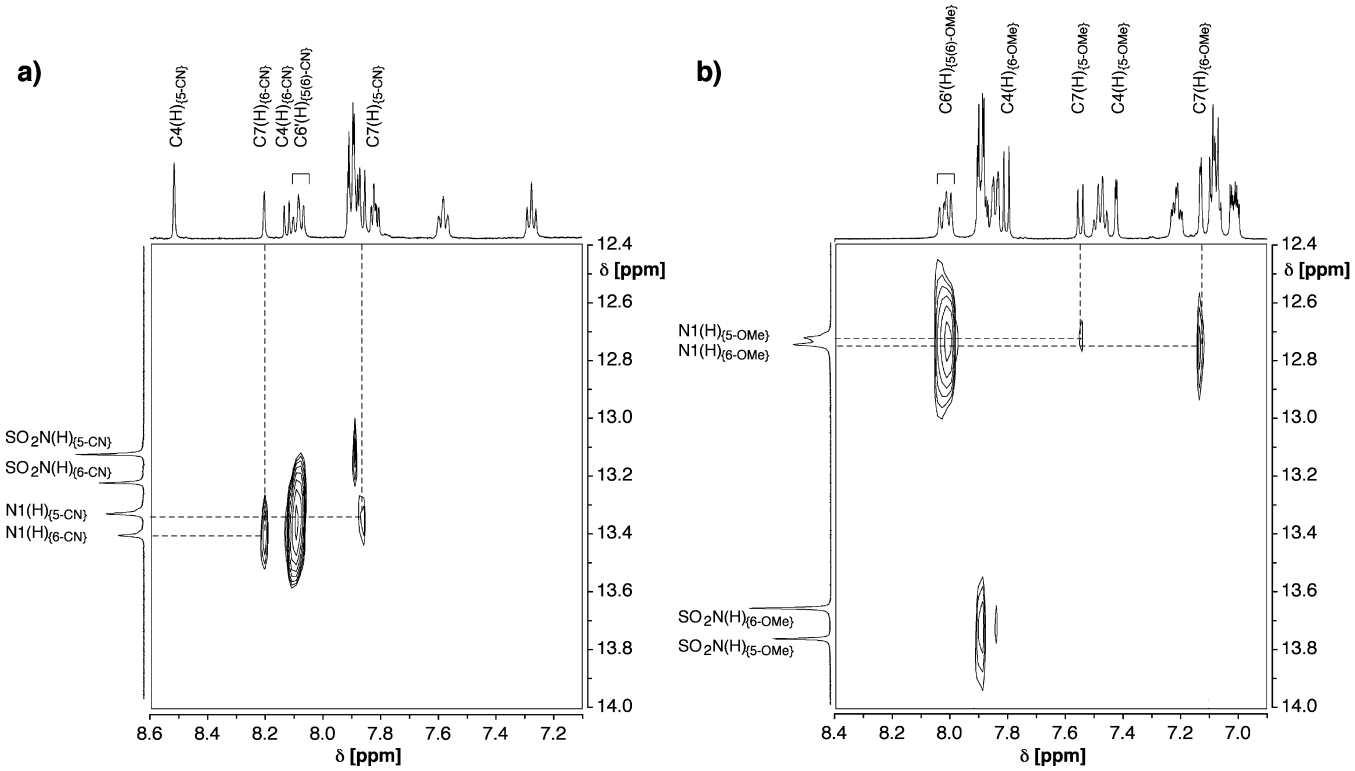

FIGURE 4. Two-dimensional 500 MHz ^{1}H−^{1}H NOESY spectra of (a) **4i** (left) and (b) **4k** (right) in acetone-d_6 at −80 °C. The dashed lines indicate the correlation signals for the benzimidazole proton N1(H) of each tautomer. For both derivatives, N1(H) shows NOE contact with the C7(H) singlet of the 6-substituted tautomer, while the 5-substituted tautomer shows an NOE contact with C(7)H appearing as a doublet (atom numbering shown in Scheme 2). Structural assignments were confirmed with 2D COSY experiments acquired at the same temperature (see the Supporting Information, Figures S1 and S2).

4. Substituent Effects on Absorption and Fluorescence Spectra. 4.1. Effect of Donor Substitution. To explore the effect of a single electron-donating substituent in relation to its attachment position on the fluorophore π-system, we first compared the UV−vis absorption and fluorescence emission spectra of the monosubstituted methoxy derivatives **5e**, **5f**, and **5k** with those of the unsubstituted parent compound **5a** (Figure 5). The deconvoluted spectra corresponding to the monoprotonated species LH^- exhibit for all four compounds a single high-energy absorption maximum (Figure 5, solid traces); however, the 4′-substituted derivative **5e** revealed an additional low-energy band centered around 360 nm (Figure 5b, left). On the basis of literature reports on structurally related compounds,[13,33] the band is most likely caused by an *inter*annular prototropic tautomer **T** (Chart 2) that is present in the ground-state equilibrium (vide infra). When substituted with a methoxy group in the 4′-position of the central benzene ring (compound **5e**), the absorption maximum of the monoprotonated species LH^- is red-shifted by 5 nm or 550 cm^{-1} (Figure 5b), while substitution in the 5′-position leads to a small blue-shift of 2 nm or 220 cm^{-1} (compound **5f**, Figure 5c) compared to the parent compound **5a**. In contrast, substitution of the benzimidazole ring with a methoxy group (compound **5k**) yields a significantly larger red-shift of 16 nm or 1690 cm^{-1} (Figure 5d).

At a proton concentration where the monoprotonated species LH^- is predominantly present (see Table 1), all four compounds exhibit a single, low-energy fluorescence emission band (Figure 5, right; solid traces). Consistent with formation of the proton-transfer species **T*** in the excited state, the peak emission of all four compounds exhibit exceptionally large Stokes shifts ranging from 9520 to 13 440 cm^{-1}. Notably, none of the derivatives exhibits dual emission, indicating that formation of the ESIPT tautomer is very efficient and neither compromised through solvent−solute hydrogen-bonding interactions,[34] solvent-polarization-induced barriers,[35] or ground-state stabilization of a rotamer that cannot undergo ESIPT.[13] Interestingly, the fluorescence maximum of monoprotonated **5k** is very similar compared to **5a**, while the 4′- and 5′-substituted derivatives **5e** and **5f** are significantly red- and blue-shifted by 28 nm (1410 cm^{-1}) and 37 nm (1620 cm^{-1}), respectively. The quantum yield of all three monomethoxy-substituted derivatives is markedly lower compared to that of their parent compound **5a** (Table 2).

To further investigate the nature of the low-energy absorption band observed for fluorophore **5e**, we studied the emission properties of this compound in more detail. Excitation into this low-energy band at 350 nm yielded an emission spectrum that was upon normalization indistinguishable from the spectrum obtained with excitation at <300 nm. Furthermore, the excitation spectrum revealed across the entire emission energy range a similar low-energy band as found in the UV−vis absorption spectrum (data not shown). These observations strongly support that fluorescence emission occurs exclusively from the proton-transfer tautomer **T***, which is to some extent already present

(33) Mosquera, M.; Penedo, J. C.; Rios Rodriguez, M. C.; Rodriguez-Prieto, F. *J. Phys. Chem.* **1996**, *100*, 5398−5407.

(34) Penedo, J. C.; Mosquera, M.; Rodriguez-Prieto, F. *J. Phys. Chem. A* **2000**, *104*, 7429−7441.

(35) Cheng, Y. M.; Pu, S. C.; Hsu, C. J.; Lai, C. H.; Chou, P. T. *ChemPhysChem* **2006**, *7*, 1372−1381.

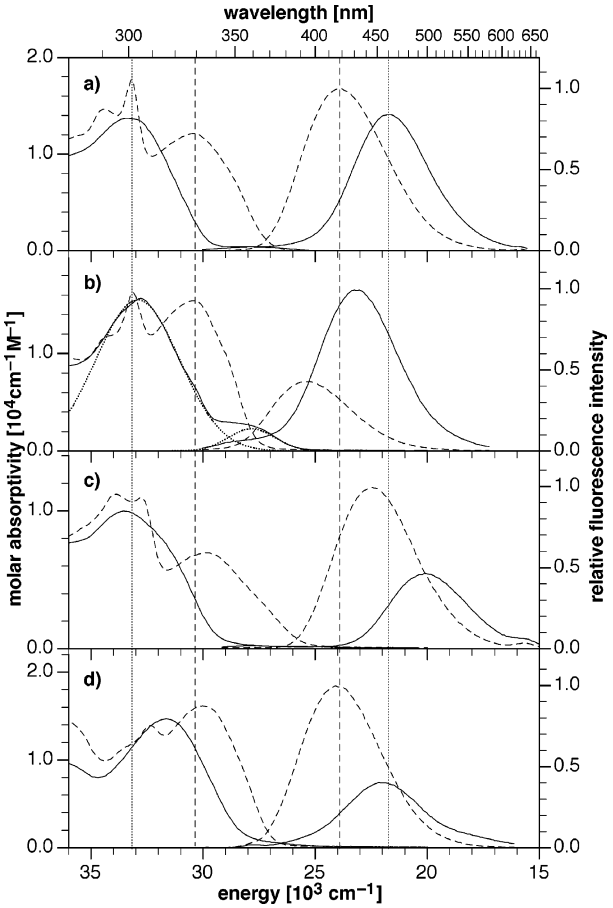

FIGURE 5. Effect of donor substituents: deconvoluted UV−vis absorption spectra (left) and fluorescence emission spectra (right) of compounds (a) **5a**, (b) **5e**, (c) **5f**, and (d) **5k** in aqueous solution (0.1 M KCl, 25 °C). UV−vis traces for the species with protonated (—) and deprotonated (- - -) sulfonamide group were obtained through deconvolution analysis of a series of spectra with $-\log[H_3O^+]$ ranging between 6 and 10. Emission spectra were acquired with excitation at the isosbestic point and were recorded near neutral pH as specified in Table 1 (—) and at pH 11 (- - -) without further deconvolution. The four vertical grid lines are added as a guide to the eye indicating the position of the peak absorption and emission of parent compound **5a**.

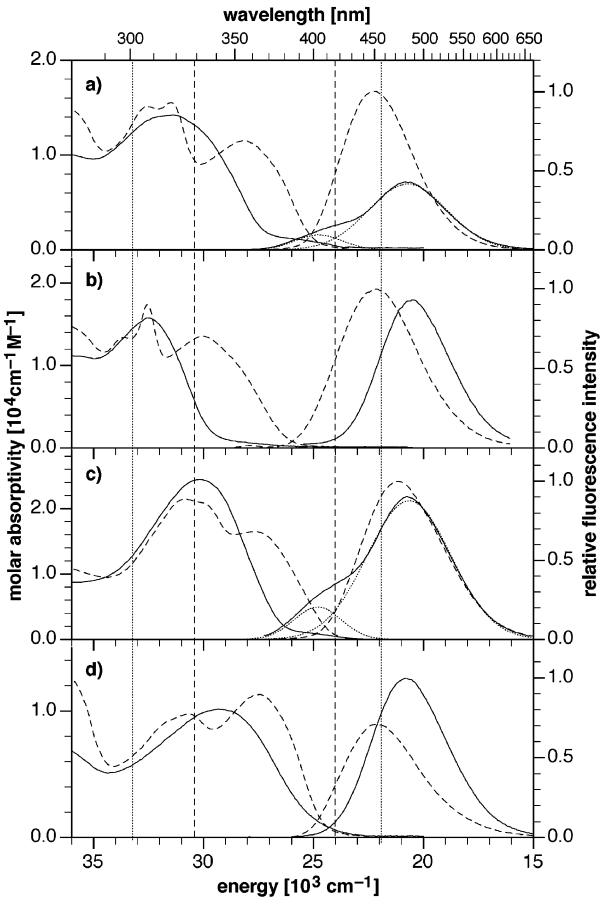

FIGURE 6. Effect of acceptor substituents: deconvoluted UV−vis absorption spectra (left) and fluorescence emission spectra (right) of compounds (a) **5b**, (b) **5i**, (c) **5d**, and (d) **5c** in aqueous solution (0.1 M KCl, 25 °C). UV−vis traces for the species with protonated (—) and deprotonated (- - -) sulfonamide group were obtained through deconvolution analysis of a series of spectra with $-\log[H_3O^+]$ ranging between 6 and 10. Emission spectra were acquired with excitation at the isosbestic point and were recorded near neutral pH as specified in Table 1 (—) and at pH 11 (- - -) without further deconvolution. The four vertical grid lines are intended as a guide to the eye indicating the position of the peak absorption and emission of parent compound **5a**.

in the ground-state equilibrium along with the normal cis-tautomer $\mathbf{N_c}$ (Chart 2).

Upon deprotonation of the sulfonamide nitrogen ($-\log[H_3O^+] > 10$), the UV−vis absorption spectra were changed dramatically (Figure 5, left, dashed traces). In comparison to the monoprotonated species LH^-, the absorption traces of all four compounds display a red-shifted band centered around 330 nm, whose energy is essentially invariable of the methoxy-substituent position. Furthermore, the spectrum of fully deprotonated **5e** reveals that the position of the lowest energy absorption band is significantly different from the low-energy band observed for its monoprotonated form, thus further corroborating formation of the interannular tautomer **T** at neutral pH.

Consistent with disruption of the ESIPT process upon sulfonamide deprotonation at high pH, all four fluorophores exhibit strongly blue-shifted emission bands with normal Stokes shifts (Figure 5, right, dashed traces). The influence of the methoxy substituents on the emission energy follows in essence the same trends as observed for the spectra of the monoprotonated species LH^-: derivative **5k** containing a methoxy group attached to the benzimidazole ring revealed again a similar spectrum compared to that of parent compound **5a**, while the peak emission of **5e** and **5f** were strongly blue- and red-shifted by 22 nm (1330 cm^{-1}) and 26 nm (1400 cm^{-1}), respectively.

Given the current data set, we can only speculate about the underlying reason for the observed divergent trends in the peak emission energies of derivative **5e** versus **5f**. As apparent from Table 2, the emission energies parallel the changes in Stokes shifts, thus indicating significant differences in the relaxation energetics of the initially formed Franck−Condon state. Since the attachment position of the methoxy group is the only structural difference between **5e** and **5f**, specific solvent−solute interactions are presumably less important. However, the attachment position could influence the degree of excited-state polarization, thus potentially leading to formation of an emissive ESIPT species with varying degree of charge-transfer character. Isotropic dipole−dipole interactions with solvent molecules would additionally pronounce such differences of the excited-state polarization. Alternatively, the methoxy substituent may differentially stabilize the frontier orbital energies of the proton-

CHART 2

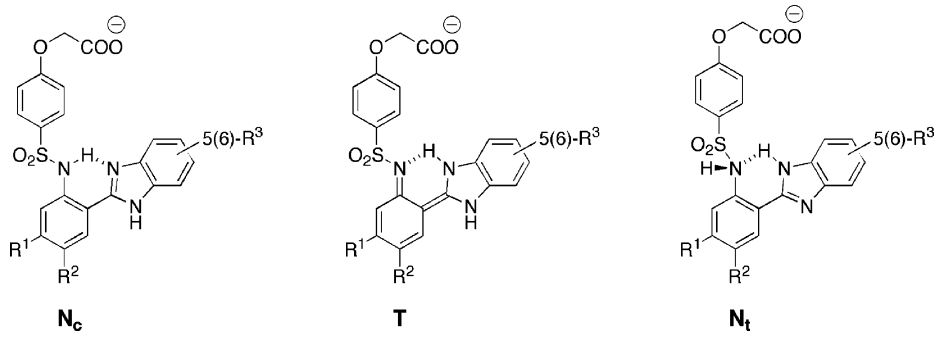

transfer species, thus leading to the divergent emission shifts. Finally, differences in the strengths of the intramolecular hydrogen bond might influence the ESIPT energetics and thus result in the observed differences of the Stokes shifts.

4.1.1. Effect of Donor Strength. To explore the influence of π-donor strength, we studied the spectral properties of the dimethylamino-substituted fluorophore **5g** in comparison with the methoxy-substituted compound **5f**. Consistent with the increased π-donor strength of the dimethylamino group compared to methoxy, the peak fluorescence wavelength of monoprotonated **5g** is strongly red-shifted by 71 nm compared to **5f**, yielding an exceptionally large Stokes shift of 14 760 cm^{-1} (Table 2). Upon deprotonation of the sulfonamide nitrogen, the fluorescence maximum of **5g** is blue-shifted by 63 nm or 2200 cm^{-1} but remains still at significantly lower energy compared to that of fully deprotonated **5f**. As previously observed for the methoxy-substituted compounds **5e**, **5f**, and **5k**, at high pH the ESIPT process is effectively disrupted, yielding emission exclusively from the fully deprotonated species L^{2-}. In comparison to **5f**, the quantum yield of **5g** is dramatically lowered at neutral pH and recovered only slightly to 8% at basic pH. Interestingly, repetitive measurements of the fluorescence emission spectrum in neutral buffered aqueous solution revealed gradual appearance of a new band, indicating significant photochemical instability under these conditions.

Although electron donation into the central aryl ring is expected to increase by derivatizing with a 4′,5′-methylenedioxy moiety (fluorophore **5l**), the spectral shifts were less dramatic (Table 2). The divergent emission energy trends observed for the two monomethoxy-substituted derivatives **5e** and **5f** appeared to be averaged out in this case. The fluorescence emission maxima and Stokes shifts fall for both the monoprotonated and fully deprotonated species of **5l** in between the values measured for **5e** and **5f**. Interestingly, the fluorescence quantum yield of **5l** is also much lower compared to that of the monosubstituted derivatives **5e** and **5f**, indicating additional nonradiative deactivation channels.

4.2. Effect of Acceptor Substitution. To assess the effect of electron-withdrawing substituents on the fluorophore properties, we explored next the photophysical properties of the cyano-substituted derivatives **5b** and **5i**. As shown in Figure 6a, compared to the parent compound **5a** the 4′-cyano-substituted derivative **5b** exhibits dramatically red-shifted absorption bands for both the monoprotonated LH^- (19 nm or 1990 cm^{-1} shift) and fully deprotonated species L^{2-} (26 nm or 2230 cm^{-1} shift). The peak emission energies are also red-shifted, but to a lesser degree, by 23 nm or 1040 cm^{-1} for LH^-, and 29 nm or 1550 cm^{-1} for L^{2-}, resulting in slightly smaller Stokes shifts compared to those of **5a**. Interestingly, the emission spectrum of the monoprotonated fluorophore reveals an additional band at higher energy, which was not observed for any of the donor-substituted derivatives (Figure 6a, right, solid trace). The overall band shape fits well to a double-Gaussian function with maxima centered at 483 (20 720 $\pm$ 10 cm^{-1}) and 404 nm (24 770 $\pm$ 30 cm^{-1}). The corresponding single-Gaussian components are shown as dotted traces in Figure 6a. On the basis of the pH at which the emission spectrum of LH^- was acquired, the estimated residual concentration of L^{2-} is less than 3% (Table 1), an amount that is too small to account for the intensity of the higher energy emission band. Furthermore, the emission spectrum of fully deprotonated L^{2-} shows a distinctly different maximum at 447 nm (Figure 6a, right, dashed trace). Conclusively, the observed higher energy fluorescence band cannot be attributed to emission from fully deprotonated L^{2-}, neither as a species formed by means of excited-state deprotonation, nor as a significant component of the ground-state equilibrium prior to excitation. Dual fluorescence is not uncommon for ESIPT fluorophores and is often due to the presence of a rotamer that cannot undergo ESIPT.[13,33] Recent quantum chemical calculations suggested, however, that the cis/trans-rotamer equilibrium for 2′-sulfonamidophenyl-substituted benzimidazoles is strongly in favor of the ESIPT capable cis-rotamer.[27] Ground-state equilibration of **5b** between the normal cis-rotamer $\mathbf{N_c}$ and the corresponding non-ESIPT trans-rotamer $\mathbf{N_t}$ is therefore rather unlikely (Chart 2). Consistent with this assumption, the normalized excitation spectra acquired at 375 and 485 nm were identical within experimental error (data not shown), suggesting that the two emissive species originate from the same ground-state structure. The observed dual emission is therefore most likely due to an excited-state process that involves competition between radiative deactivation of the normal tautomer $\mathbf{N_c}$* and formation of the phototautomer **T*** through ESIPT. It appears that the electron-withdrawing cyano substituent in **5b** adversely affects the rate of ESIPT, possibly through an unfavorable change of the excited-state acidity of the sulfonamide proton[36] or through a substantially different polarization between vibrationally equilibrated **T*** and $\mathbf{E_c}$*. The latter scenario would yield a solvent-polarization-induced barrier of the ESIPT process, and thus an excited-state equilibrium between the phototautomer **T*** and the normal tautomer $\mathbf{N_c}$*, resulting in competitive radiative deactivation of both species.[35]

In contrast, derivative **5i** substituted with a cyano group at the benzimidazole ring lacks the higher energy emission band and exhibits solely fluorescence from the ESIPT tautomer

(36) Doroshenko, A. O.; Posokhov, E. A.; Verezubova, A. A.; Ptyagina, L. M. *J. Phys. Org. Chem.* **2000**, *13*, 253−265.

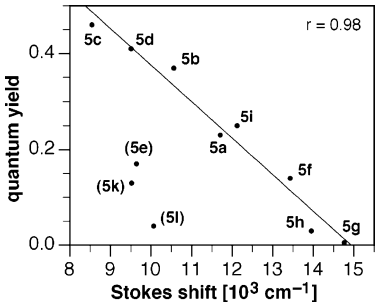

FIGURE 7. Linear correlation between Stokes shift and quantum yield for the monoprotonated fluorophores **5a-5l** (r = correlation coefficient; **5e**, **5k**, and **5l** were excluded from the correlation).

(Figure 6b). The peak emission energy is also red-shifted relative to that of unsubstituted **5a** and very similar compared to that of **5b**. At high pH, the fully deprotonated species L^{2-} emits at almost identical energy compared to **5b**, though with significantly lower quantum yield. The UV−vis maxima at basic and neutral pH are both red-shifted compared to those of the parent compound **5a**, but to a lesser degree than those of **5b**, thus resulting in larger Stokes shifts.

While acting also as an electron-withdrawing substituent, the thiazolyl ring in **5d** naturally extends the π-system of the parent fluorophore. This is best reflected by the fact that the absorption maxima of **5d** are even more red-shifted compared to those of **5i** (Figure 6c), although the sulfonamide pK_a is lowered to a lesser degree by thiazolyl compared to cyano substitution (Table 1). As already observed for fluorophore **5b**, the emission spectrum of monoprotonated **5d** reveals two bands, which fit well to a double-Gaussian function with maxima centered at 484 nm (20 650 ± 10 cm^{-1}) and 403 nm (24 810 cm^{-1} ± 30 cm^{-1}). Analogous to **5b**, the normalized excitation spectra acquired at 403 and 484 nm exhibit no differences within experimental error (data not shown), suggesting that the dual emission is again due to competing excited-state processes rather than ground-state equilibration between cis- and trans-rotamers.

Deprotonation of the sulfonamide nitrogen yields again a single emission band; however, the observed blue-shift is with 9 nm (390 cm^{-1}) substantially smaller compared to that of **5b**. As evident from Table 2, this reduction is mainly a consequence of the decreased Stokes shift of the lower energy band in **5d** compared to **5b**, rather than anomalous emission behavior of the fully deprotonated species.

4.3. Effect of Donor−Acceptor Double Substitutions. Double substitution with a donor and acceptor group has the potential to increase the charge-transfer character in the ground and excited state, which in turn might lead to further red-shifted absorption and emission spectra. To explore the effect of such modifications, we studied the spectral properties of derivative **5c** and **5h**, both containing a methoxy and cyano group in opposing positions of the fluorophore framework. As shown in Figure 6d, compared to unsubstituted **5a** fluorophore **5c** exhibits indeed strongly red-shifted absorption bands for both the monoprotonated species LH^- (41 nm or 4010 cm^{-1} shift) and fully deprotonated L^{2-} (33 nm or 2770 cm^{-1} shift). The emission band of the former species peaks at 481 nm, corresponding to a 21 nm (950 cm^{-1}) red-shift compared to **5a**. Interestingly, ESIPT is very efficient in **5c** and results in a single emission band without the high-energy component found for **5b**. Although the Stokes shift for the ESIPT emission is the smallest among all studied compounds, deprotonation of the sulfonamide still resulted in a significantly blue-shifted emission band (29 nm or 1330 cm^{-1}). It is noteworthy that the quantum yield of monoprotonated **5c** is with 46% 2-fold greater than for **5a** and the highest of all studied compounds.

While the double-substitution pattern in **5c** resulted in improved photophysical properties compared to the corresponding monosubstituted counterparts, fluorophore **5h** revealed low quantum yields regardless of the protonation state. Nevertheless, the compound exhibits qualitatively the same behavior with a large Stokes-shifted emission for the monoprotonated species and normal emission at high pH.

4.4. Quantum Yields. The fluorescence quantum yield of the ESIPT tautomer appears to correlate significantly with the observed Stokes shift. As illustrated in Figure 7, with exception of the methoxy-substituted derivatives **5e**, **5k**, and **5l**, the quantum yields linearly decrease with increasing Stokes shifts (correlation coefficient r = 0.984). The data suggest that the degree of excited-state reorganization and geometrical relaxation in the course of the proton-transfer process is an important factor that determines the fluorescence efficiency in competition with nonradiative deactivation processes. It is noteworthy that no appreciable correlation was found regarding the trends in emission energies of the ESIPT species, indicating that the quantum yield trends are not just a reflection of the energy gap rule.

Concluding Remarks

The primary motivation for this study was to explore whether donor and acceptor substituents are capable of shifting the peak absorption and emission wavelength of 2-(2′-arylsulfonamidophenyl)benzimidazole fluorophores toward lower energy, an important aspect in light of biological imaging applications. Standard fluorescence microscopes are typically equipped with optics that are not transmissible below 350 nm, thus hampering unsubstituted **5a** as a fluorophore platform for biological sensing applications. In this context, several of the studied substituted derivatives were found to meet this requirement. Notably, derivatives **5c** and **5d** exhibit strongly red-shifted absorption bands. Upon deprotonation at basic pH, both compounds revealed isosbestic points that also match the desired wavelength criteria (Table 2), making it possible to excite the mono- and fully deprotonated form with equal efficiency. In addition, derivative **5c** stands out due to its high quantum yield and a significant blue-shift of the fluorescence emission upon deprotonation.

All derivatives yielded emission from the ESIPT tautomer **T***; however, fluorophore **5b** and **5d** revealed an additional higher energy band that is most likely due to emission from the normal tautomer $\mathbf{N_c}$*. While alteration of the fluorophore π-system can be used to effectively tune the ESIPT emission energy, this strategy unavoidably carries also the risk of reducing the rate of ESIPT and thus of introducing additional, competing radiative deactivation channels. Further complications might arise from hydrogen-bonding interactions with solvent molecules and/or the presence of rotamers that cannot undergo ESIPT. The prediction of such excited-state processes remains a challenging task based on simple structural arguments; however, the results of this study may provide guidelines for tuning the

properties of this class of fluorophores to design emission ratiometric pH or metal-cation sensors for biological applications.

Experimental Section

Synthesis. Benzimidazole derivatives **4a** and **5a**, (4-chlorosulfonyl-phenoxy)acetic acid ethyl ester **10**, and 2-(4-(*N*-(2-formylphenyl)sulfamoyl)phenoxy)acetic acid ethyl ester **9i** were synthesized as previously described.[14] Compounds 4-cyano-2-nitrobenzaldehyde[37] (**1b**), 5-methoxy-2-nitrobenzaldehyde[38] (**1f**), 4-methoxy-2-nitrobenzaldehyde[39] (**1e**), and 4-bromo-2-nitrobenzaldehyde[40] were synthesized according to published procedures. NMR: δ in ppm versus $SiMe_4$ (0 ppm, ^1H, 400 MHz; 0 ppm, ^{13}C, 100 MHz). Note: due to the presence of prototropic exchange equilibria, benzimidazole hydrogens are in many cases broadened (indicated as "br") or not resolved. Similarly, ^{13}C resonances for C3a(7a), C4(7), and C5(6) of the benzimidazole ring were either broadened or absent. For variable temperature NMR experiments, the actual sample temperature was determined by means of a calibration curve using neat methanol as chemical-shift thermometer.[41] Two-dimensional NOESY $^1H-^1H$ NMR spectra were acquired in acetone-d_6 at 193 K with a 500 MHz spectrometer (300 ms mixing time). Structural assignments of the observed signals were made on the basis of 2D COSY experiments acquired at the same temperature (see the Supporting Information, Figures S1 and S2). MS: selected peaks; *m*/*z*. Melting points are uncorrected. Flash chromatography (FC): silica gel (240−400 mesh).

2-Nitro-4-(thiazol-2-yl)benzaldehyde (1d). A solution of 4-bromo-2-nitrobenzaldehyde[40] (310 mg, 1.3 mmol), 2-(tributylstannyl)-thiazole (500 mg, 410 μL, 1.3 mmol), and $Pd(PPh_3)_4$ (50 mg, 0.043 mmol) in DMF (10 mL) was degassed and then heated at 80 °C overnight. After cooling to room temperature, the reaction mixture was diluted with CH_2Cl_2, washed with deionized water, and concentrated under reduced pressure. The residual crude product was purified on silica gel (FC, EtOAc/hexanes, 1:3) providing 340 mg (1.45 mmol, quantitative yield) of thiazole **1d** as a yellow solid. Mp 101−103 °C; ^1H NMR ($CDCl_3$, 400 MHz) δ 7.55 (d, J = 3.1 Hz, 1H), 8.01 (d, J = 3.2 Hz, 1H), 8.06 (d, J = 8.0 Hz, 1H), 8.34 (dd, J = 8.0 Hz, 1.7 Hz, 1H), 8.71 (d, J = 1.7 Hz, 1H), 10.45 (s, 1H); ^{13}C NMR ($CDCl_3$, 100 MHz) δ 121.6, 122.0, 130.4, 130.87, 130.91, 138.6, 144.8, 150.1, 163.8, 187.3; IR (KBr) 3121, 3106, 2926, 1691, 1526, 1506, 1348, 1141, 824, 770, 736 cm^{-1}; MS (70 eV) *m*/*z* 234 ([M$^+$], 11), 204 (100), 176 (25), 159 (27); EI-HRMS calcd for $C_{10}H_6N_2O_3S$ 234.0099, found 234.0078.

5-(Dimethylamino)-2-nitrobenzaldehyde (1g). A mixture of 5-fluoro-2-nitrobenzaldehyde (100 mg, 0.59 mmol), dimethylamine hydrochloride (77 mg), and anhydrous K_2CO_3 (245 mg) in DMSO (2 mL) was heated at 105 °C for 2 h. After cooling to room temperature, the reaction mixture was diluted with water, and the precipitated product was extracted twice with diethylether (40 mL). The combined organic extracts were dried with anhydrous $MgSO_4$, filtered, and concentrated under reduced pressure, providing 92 mg (0.47 mmol, 80% yield) of compound **1g** as a yellow solid. Mp 124−126 °C; ^1H NMR ($CDCl_3$, 400 MHz) δ 3.16 (s, 6H), 6.72 (dd, J = 9.3, 3.0 Hz, 1H), 6.91 (d, J = 3.0 Hz, 1H), 8.11 (d, J = 9.3 Hz, 1H), 10.51 (s, 1H); ^{13}C NMR ($CDCl_3$, 100 MHz) δ 40.3, 110.0, 112.7, 127.4, 135.0, 136.2, 153.3, 190.0; IR (KBr) 2902, 1701, 1600, 1573, 1295, 1261, 1231, 1198, 886, 811 cm^{-1}; MS (70 eV) *m*/*z* 194.1 ([M$^+$], 100), 164.1 (18), 136.3 (100), 119.1 (32), 105.1 (18); EI-HRMS calcd for [M$^+$] $C_9H_{10}N_2O_3$ 194.0691, found 194.0674.

General Procedure A: Synthesis of Benzimidazole Derivatives through Oxidative Coupling with Benzoquinone. An equimolar solution of the corresponding aldehyde and phenylenediamine (0.5 mmol) in EtOH (2 mL) was heated under reflux until all starting material was converted to the imine intermediate (ca. 1.5 h). After addition of 1,4-benzoquinone (119 mg, 1.10 mmol) the reaction mixture was heated at reflux until the imine intermediate was completely converted to the benzimidazole product (typically 30−60 min). The reaction mixture was then cooled to room temperature, diluted with saturated aqueous $NaHCO_3$, and the product was extracted twice with ethyl acetate. The combined organic extracts were dried with anhydrous $MgSO_4$, filtered, and concentrated under reduced pressure. The crude product was purified by FC on silica to give the analytically pure benzimidazole.

4-(1*H*-Benzimidazol-2-yl)-3-nitrobenzonitrile (2b). Starting from 200 mg of aldehyde **1b** (0.12 mmol) and 1,2-phenylenediamine (129 mg, 1.19 mmol), benzimidazole derivative **2b** was obtained in 43% yield (FC, EtOAc/hexanes, gradient 1:2 to 1:1). Mp 209−211 °C; ^1H NMR (CD_3OD, 400 MHz) δ 7.33 (m, 2H), 7.64 (br, 2H), 8.06 (d, J = 8.2 Hz, 1H), 8.20 (dd, J = 8.2, 1.6 Hz, 1H), 8.53 (d, J = 1.6 Hz, 1H); ^{13}C NMR (acetone-d_6, 100 MHz) δ 115.7, 117.2, 124.5 (br), 129.5, 130.1, 133.7, 137.1, 147.5, 150.0; IR (KBr) 3198, 3097, 3072, 2236, 1560, 1535, 1425, 1354, 787, 747 cm^{-1}; MS (70 eV) *m*/*z* 264.1 ([M$^+$], 100), 247.1 (65), 234.1 (26); EI-HRMS calcd for [M$^+$] $C_{14}H_8N_4O_2$ 264.06473, found 264.06592.

4-(5(6)-Methoxy-1*H*-benzimidazol-2-yl)-3-nitrobenzonitrile (2c). Starting from 200 mg of aldehyde **1b** (0.12 mmol) and 4-methoxybenzene-1,2-diamine (165 mg, 1.19 mmol), benzimidazole derivative **2c** was obtained in 30% yield (FC, EtOAc/hexanes, gradient 1:2 to 1:1). Mp 75−77 °C; ^1H NMR (CD_3OD, 400 MHz) δ 3.86 (s, 3H), 6.95 (dd, J = 8.9, 2.4 Hz, 1H), 7.09 (br, 1H), 7.52 (d, J = 8.7 Hz, 1H), 8.02 (d, J = 8.0 Hz, 1H), 8.16 (dd, J = 8.0, 1.6 Hz, 1H), 8.49 (d, J = 1.6 Hz, 1H); ^{13}C NMR (acetone-d_6, 100 MHz) δ 55.9, 114.0, 114.2, 117.1, 128.5, 128.7, 131.9, 136.0, 145.3, 149.6, 157.9; IR (KBr) 3074, 2946, 2234, 1617, 1540, 1269, 1198, 1157, 1025, 1001, 831 cm^{-1}; MS (70 eV) *m*/*z* 294.1 ([M$^+$], 100); EI-HRMS calcd for [M$^+$] $C_{15}H_{10}N_4O_3$ 294.07529, found 294.07582.

2-(2-Nitro-4-thiazol-2-yl-phenyl)-1*H*-benzimidazole (2d). Starting from 28 mg of aldehyde **1d** (0.12 mmol) and 1,2-phenylenediamine (15 mg, 0.14 mmol), benzimidazole derivative **2d** was obtained in 31% yield (FC, EtOAc/hexanes, 1:1). Mp 120−122 °C; ^1H NMR ($CD_3OD/CDCl_3$ 1:1, 400 MHz) δ 7.29−7.35 (m, 2H), 7.61−7.68 (br, 2H), 7.69 (d, J = 3.2 Hz, 1H), 7.96 (d, J = 8.1 Hz, 1H), 8.00 (d, J = 3.2 Hz, 1H), 8.33 (dd, J = 8.1, 1.8 Hz, 1H), 8.65 (d, J = 1.8 Hz, 1H); ^{13}C NMR ($CD_3OD/CDCl_3$, 100 MHz) δ 122.1, 123.0, 123.9 (br), 126.9, 130.8, 133.5, 136.5, 144.9, 148.2, 150.0, 165.6; IR (KBr) 3120, 3091, 1534, 1518, 1474, 1448, 1433, 1369, 1354, 1276, 771, 746 cm^{-1}; MS (70 eV) *m*/*z* 322 ([M$^+$], 50), 292 (100), 129 (57), 57(52), 40.9 (37); EI-HRMS calcd for [M$^+$] $C_{16}H_{10}N_4O_2S$ 322.0525, found 322.0496.

2-(4-Methoxy-2-nitro-phenyl)-1*H*-benzimidazole (2e). Starting from 410 mg of aldehyde **1e** (2.26 mmol) and 1,2-phenylenediamine (257 mg, 2.37 mmol), benzimidazole derivative **2e** was obtained in 82% yield (FC, EtOAc/hexanes, gradient 1:4 to 1:2). Mp 178−180 °C; ^1H NMR (CD_3OD, 400 MHz) δ 3.96 (s, 3H), 7.25−7.29 (m, 2H), 7.38 (dd, J = 8.6, 2.6 Hz, 1H), 7.58 (br, 2H), 7.65 (d, J = 2.6 Hz, 1H), 7.74 (d, J = 8.6 Hz, 1H); ^{13}C NMR (DMSO-d_6, 100 MHz) δ 56.3, 109.6, 115.9, 117.8, 122.1 (br), 131.6, 147.1, 149.7, 160.1; IR (KBr) 2844, 1628, 1531, 1500, 1449, 1430, 1304, 1272, 1238, 1027, 755 cm^{-1}; MS (70 eV) *m*/*z* 269 ([M$^+$], 90), 239.1 (100), 196 (32), 110.1 (77); EI-HRMS calcd for [M$^+$] $C_{14}H_{11}N_3O_3$ 269.0800, found 269.0816.

3-Amino-4-(1*H*-benzimidazol-2-yl)benzonitrile (3b). A solution of nitro-substituted benzimidazole intermediate **2b** (102 mg, 0.39

(37) Dann, O.; Ruff, J.; Wolff, H. P.; Griessmeier, H. *Liebigs Ann. Chem.* **1984**, 409−425.
(38) Manetsch, R.; Zheng, L.; Reymond, M. T.; Woggon, W.-D.; Reymond, J.-L. *Chem. Eur. J.* **2004**, *10*, 2487−2506.
(39) Katritzky, A. R.; Xu, Y.-J.; Vakulenko, A. V.; Wilcox, A. L.; Bley, K. R. *J. Org. Chem.* **2003**, *68*, 9100−9104.
(40) Jung, M. E.; Dansereau, S. M. K. *Heterocycles* **1994**, *39*, 767−778.
(41) Amman, C.; Meier, P.; Merbach, A. E. *J. Magn. Reson.* **1982**, *46*, 319−321.

mmol) in 5 mL of methanol was hydrogenated at room temperature under ambient pressure in the presence of Pd on activated carbon as catalyst (25 mg, 5 wt % Pd). After completion of the reaction (TLC), the catalyst was filtered off through a pad of Celite, and the filtrate was concentrated under reduced pressure providing 85 mg (0.36 mmol, 94% yield) of amine **3b** as a yellow solid. Mp 88−90 °C; ^{1}H NMR (CD_3OD, 400 MHz) δ 6.92 (dd, J = 8.2, 1.6 Hz, 1H), 7.12 (d, J = 1.6 Hz, 1H), 7.22−7.25 (m, 2H), 7.58 (br, 2H), 7.79 (d, J = 8.2 Hz, 1H); ^{13}C NMR (CD_3OD, 100 MHz) δ 114.0, 116.0, 119.1, 119.7, 120.1, 129.0, 149.2, 151.9; IR (KBr) 3305 (br), 3060, 2228, 1617, 1586, 1577, 1454, 1437, 1334, 1267, 766, 741 cm^{-1}; MS (70 eV) m/z 234.1 ([M$^+$], 100); EI-HRMS calcd for [M$^+$] $C_{14}H_{10}N_4$ 234.0906, found 234.0907.

3-Amino-4-(1*H*-benzimidazol-2-yl)benzonitrile (3c). Synthesized from **2c** as described for **3b**, 53% yield. Mp 193−195 °C; ^{1}H NMR (CD_3OD, 400 MHz) δ 3.83 (s, 3H), 6.87 (dd, J = 8.8, 2.7 Hz, 1H), 6.93 (dd, J = 8.2, 1.6 Hz, 1H), 7.07 (d, J = 2.2 Hz, 1H), 7.12 (d, J = 1.6 Hz, 1H), 7.49 (d, J = 8.8 Hz, 1H), 7.79 (d, J = 8.2 Hz, 1H); ^{13}C NMR (CD_3OD, 100 MHz) δ 56.2, 97.6, 113.3, 113.5, 116.2, 117.3, 119.0, 119.9, 128.7, 135.4, 139.3, 148.9, 151.6, 157.9; IR (KBr) 3296, 2224, 1631, 1610, 1590, 1453, 1434, 1338, 1263, 1199, 1158, 832 cm^{-1}; MS (70 eV) m/z 264 ([M$^+$], 100), 249.1 (52), 167 (28), 147.9 (78), 129 (90); EI-HRMS calcd for [M$^+$] $C_{15}H_{12}N_4O$ 264.1011, found 264.1014.

2-(1*H*-Benzimidazol-2-yl)-5-thiazol-2-yl-phenylamine (3d). Synthesized from **2d** as described for **3b**, 88% yield. Mp dec >230 °C; ^{1}H NMR (CD_3OD, 400 MHz) δ 7.12−7.16 (m, 2H), 7.21 (dd, J = 8.2, 1.8 Hz, 1H), 7.37 (d, J = 1.8 Hz, 1H), 7.47−7.52 (m, 2H), 7.53 (d, J = 3.3 Hz, 1H), 7.73 (d, J = 8.2 Hz, 1H), 7.79 (d, J = 3.3 Hz, 1H); ^{13}C NMR (CD_3OD, 100 MHz) δ 114.2, 114.7, 115.1 (br), 115.3, 120.1, 123.0, 128.9, 135.1, 139.9 (br), 143.6, 148.3, 152.3, 169.4; IR (KBr) 3321, 2500, 1617, 1452, 1286, 1262, 1138, 1060, 868, 806, 730, 658 cm^{-1}; FAB-MS (thioglycerol) m/z 293 ([M$^+$], 100), 237 (13); FAB-HRMS calcd for [M$^+$] $C_{16}H_{13}N_4S$ 293.0861, found 293.0876.

2-(4-Methoxy-2-amino-phenyl)-1*H*-benzimidazole (3e). Synthesized from **2e** as described for **3b**, 99% yield (FC, hexanes/EtOAc, gradient 3:1 to 2:1). Mp 140−143 °C; ^{1}H NMR (DMSO-d_6, 400 MHz) δ 3.74 (s, 3H), 6.27 (dd, J = 8.7, 2.4 Hz, 1H), 6.37 (d, J = 2.4 Hz, 1H), 7.11−7.18 (m, 2H), 7.32 (br, 2H), 7.45 (d, J = 7.3 Hz, 1H), 7.59 (d, J = 7.3 Hz, 1H), 7.76 (d, J = 8.7 Hz, 1H), 12.47 (s, 1H); ^{13}C NMR (DMSO-d_6, 100 MHz) δ 54.8, 99.2, 102.7, 103.7, 110.3, 117.6, 121.0, 121.7, 128.4, 133.2, 142.8, 149.6, 149.7, 152.4, 160.9; IR (KBr) 3201, 1627, 1614, 1502, 1447, 1431, 1251, 1214, 1026, 735 cm^{-1}; MS (70 eV) m/z 239 ([M$^+$], 100), 210 (7), 196 (32); EI-HRMS calcd for [M$^+$] $C_{14}H_{13}N_3O$ 239.1058, found 239.1056.

2-(4-(*N*-(2-(1*H*-Benzimidazol-2-yl)-5-cyanophenyl)sulfamoyl)-phenoxy)acetic Acid Ethyl Ester (4b). To a solution of amine **3b** (35 mg, 0.149 mmol) in anhydrous pyridine (2 mL) was added (4-chlorosulfonyl-phenoxy)-acetic acid ethyl ester[14] **10** (50 mg, 0.179 mmol). After stirring at room temperature for 18 h, the reaction mixture was poured into aqueous 1 M HCl (20 mL), and the product was extracted twice with ethyl acetate. The combined organic extracts were dried with anhydrous $MgSO_4$, filtered, and concentrated under reduced pressure. The crude product was purified on silica gel (EtOAc/hexanes, gradient 1:3 to 1:1) providing 25 mg (0.053 mmol, 35%) of sulfonamide **4b** as a tan solid. Mp 208−210 °C; ^{1}H NMR ($CDCl_3$, 400 MHz) δ 1.34 (t, J = 7.1 Hz, 3H), 4.31 (q, J = 7.1 Hz, 2H), 4.65 (s, 2H), 6.45 (d, J = 9.0 Hz, 2H), 7.34−7.40 (m, 4H), 7.43 (dd, J = 8.1 Hz, 1.6 Hz, 1H), 7.50 (br, 1H), 7.58 (d, J = 8.0 Hz, 1H), 7.83 (br, 1H), 8.05 (d, J = 1.5 Hz, 1H), 9.93 (s, 1H), 12.18 (s, 1H); ^{13}C NMR ($CDCl_3$/acetone-d_6, 100 MHz) δ 13.7, 61.2, 64.7, 112.9, 114.2, 117.4, 119.9, 122.3, 123.3 (br), 125.9, 126.9, 128.7, 131.2, 137.6, 147.9, 160.6, 167.4; IR (KBr) 3313, 3068, 2983, 2232, 1757, 1595, 1497, 1403, 1277, 1226, 1155, 1095, 555 cm^{-1}; MS (70 eV) m/z 476.1 ([M$^+$], 39), 412.1 (35), 325.1 (37), 233.1(100); EI-HRMS calcd for [M$^+$] $C_{24}H_{20}N_4O_5S$ 476.1154, found 476.1156.

2-(4-(*N*-(5-Cyano-2-(5(6)-methoxy-1*H*-benzimidazol-2-yl)phenyl)sulfamoyl)phenoxy)acetic Acid Ethyl Ester (4c). Synthesized from amine **3c** as described for **4b**, 43% yield. Mp 83−85 °C; ^{1}H NMR (CD_3OD) δ 1.20 (t, J = 7.1 Hz, 3H), 3.87 (s, 3H), 4.17 (q, J = 7.1 Hz, 2H), 4.65 (s, 2H), 6.81 (d, J = 9.0 Hz, 2H), 6.97 (dd, J = 8.9, 2.4 Hz, 1H), 7.11 (d, J = 2.3 Hz, 1H), 7.49 (dd, J = 8.2, 1.6 Hz, 1H), 7.57 (d, J = 8.9 Hz, 1H), 7.64 (d, J = 9.0 Hz, 2H), 7.92 (d, J = 8.2 Hz, 1H), 7.98 (d, J = 1.5 Hz, 1H); ^{13}C NMR (DMSO-d_6/$CDCl_3$, 100 MHz) δ 13.6, 55.1, 60.7, 64.5, 111.9, 113.1 (br), 114.2, 117.4, 119.6, 121.2, 125.5, 127.0, 128.3, 130.9, 137.0, 147.4, 156.4, 160.4, 166.9; IR (KBr) 3400, 2980, 2231, 1759, 1595, 1496, 1400, 1273, 1200, 1158, 1095, 828, 554 cm^{-1}; MS (70 eV) 506.1 ([M$^+$], 47), 263.1 (100); EI-HRMS m/z calcd for [M$^+$] $C_{25}H_{22}N_4O_6S$ 506.1260, found 506.1281.

(4-(2-(1*H*-Benzimidazol-2-yl)-5-thiazol-2-yl-phenylsulfamoyl)-phenoxy)-acetic Acid Ethyl Ester (4d). Synthesized from amine **3d** as described for **4b**, yield 68% (FC, EtOAc/hexanes, 1:1). Mp 202−204 °C; ^{1}H NMR (CD_3OD/$CDCl_3$ 1:1, 400 MHz) δ 1.23 (t, J = 7.1 Hz, 3H), 4.20 (q, J = 7.1 Hz, 2H), 4.59 (s, 2H), 6.76 (d, J = 9.0 Hz, 2H), 7.30−7.36 (m, 2H), 7.57 (d, J = 3.3 Hz, 1H), 7.64−7.71 (m, 2H), 7.74 (d, J = 9.0 Hz, 2H), 7.77 (dd, J = 8.3, 1.8 Hz, 1H), 7.91 (d, J = 3.3 Hz, 1H), 7.93 (d, J = 8.3 Hz, 1H), 8.29 (d, J = 1.7 Hz, 1H); ^{13}C NMR (CD_3OD/$CDCl_3$ 1:1, 100 MHz) δ 14.2, 62.2, 65.5, 115.1, 119.0, 119.3, 120.8, 121.9, 123.8, 128.1, 129.9, 132.2, 135.3, 138.6, 144.2, 150.3, 161.7, 168.0, 169.1; IR (KBr) 2923, 2852, 2265, 1775, 1758, 1594, 1577, 1497, 1406, 1330, 1151, 654, 573, 555 cm^{-1}; MS (70 eV) m/z 534 ([M$^+$], 48), 470 (13), 383 (24), 291 (100); EI-HRMS calcd for [M$^+$] $C_{26}H_{22}N_4O_5S_2$ 534.1032, found 534.1023.

(4-(2-(1*H*-Benzimidazol-2-yl)-5-methoxy-phenylsulfamoyl)-phenoxy)-acetic Acid Ethyl Ester (4e). Synthesized from amine **3e** as described for **4b**, 36% yield (FC, hexanes/EtOAc, gradient 2:1 to 1:1). Mp 75−77 °C; ^{1}H NMR ($CDCl_3$, 400 MHz) δ 1.28 (t, J = 7.1 Hz, 3H), 3.71 (s, 3H), 4.25 (q, J = 7.1 Hz, 2H), 4.57 (s, 2H), 6.53 (d, J = 8.9 Hz, 2H), 6.57 (d, J = 2.5 Hz, 1H), 7.20 (d, J = 2.5 Hz, 1H), 7.22−7.26 (m, 2H), 7.42 (d, J = 8.7 Hz, 1H), 7.50 (br, 2H), 7.52 (d, J = 8.9 Hz, 2H), 7.75 (br, 1H), 9.88 (br, 1H); ^{13}C NMR ($CDCl_3$, 100 MHz) δ 14.2, 29.8, 55.5, 61.9, 64.8, 106.8, 110.5, 110.7 (br), 111.0, 114.0, 118.9 (br), 122.9 (br), 127.4, 128.9, 131.3, 132.8 (br), 138.7, 142.2 (br), 149.8, 160.4, 161.0, 168.2; IR (KBr) 3367, 2925, 1754, 1596, 1582, 1497, 1409, 1274, 1200, 1143, 1094, 1082, 585 cm^{-1}; MS (70 eV) m/z 481 ([M$^+$], 46), 330 (21), 238 (100); EI-HRMS calcd for [M$^+$] $C_{24}H_{23}N_3O_6S$ 481.1308, found 481.1297.

Imidazole derivatives **4f**−**l** were synthesized according to procedure A.

4-(2(1*H*-Benzimidazol-2-yl)-4-methoxy-phenylsulfamoyl)-phenoxy-acetic Acid Ethyl Ester (4f). Starting from 50 mg of aldehyde **9f** (0.13 mmol) and 1,2-phenylenediamine (15 mg, 0.13 mmol), benzimidazole **4f** was obtained in 74% yield (FC, EtOAc/hexanes, gradient 1:4 to 1:2). Mp 76−78 °C; ^{1}H NMR ($CDCl_3$, 400 MHz) δ 1.38 (t, J = 7.1 Hz, 3H), 3.83 (s, 3H), 4.36 (q, J = 7.1 Hz, 2H), 4.65 (s, 2H), 6.13 (d, J = 8.9, 2H), 6.89 (d, J = 2.9 Hz, 1H), 6.95 (d, J = 8.9 Hz, 2H), 6.97 (dd, J = 8.9, 2.9 Hz, 1H), 7.29−7.34 (m, 2H), 7.43 (br, 1H), 7.71 (d, J = 8.9, 1H), 7.78 (br, 1H), 9.76 (s, 1H), 10.68 (s, 1H); ^{13}C NMR ($CDCl_3$, 100 MHz) δ 14.2, 55.6, 62.0, 64.4, 111.2 (br), 112.0, 113.3, 115.6, 119.1 (br), 122.4, 122.6 (br), 123.5 (br), 126.8, 128.5, 129.4, 130.0, 133.2 (br), 133.6, 149.1, 157.0, 160.0, 168.7; IR (KBr) 3338, 2936, 1757, 1735, 1595, 1502, 1325, 1279, 1214, 1158, 1094, 831, 566 cm^{-1}; MS (70 eV) m/z 481 ([M$^+$], 38), 238 (100); EI-HRMS calcd for [M$^+$] $C_{24}H_{23}N_3O_6S$ 481.1307, found 481.1320.

2-(4-(*N*-(2-(1*H*-Benzimidazol-2-yl)-4-(dimethylamino)phenyl)-sulfamoyl)phenoxy)acetic Acid Ethyl Ester (4g). Starting from 131 mg of aldehyde **9g** (0.32 mmol) and 1,2-phenylenediamine (26 mg, 0.20 mmol), benzimidazole **4g** was obtained in 50% yield (FC, EtOAc/hexanes, gradient 1:3 to 1:1). Mp 82−84 °C; ^{1}H NMR (CD_3-OD, 400 MHz) δ 1.17 (t, J = 7.1 Hz, 3H), 2.89 (s, 6H), 4.13 (q, J = 7.1 Hz, 2H), 4.43 (s, 2H), 6.40 (d, J = 8.8 Hz, 2H), 6.73 (dd,

J = 9.3, 2.7 Hz, 1H), 6.97 (d, J = 3.3 Hz, 1H), 7.20−7.26 (m, 4H), 7.48 (d, J = 9.3 Hz, 1H), 7.55 (br, 2H); ^{13}C NMR ($CDCl_3$, 100 MHz) δ 14.2, 40.4, 61.8, 64.3, 109.7, 113.2, 114.1, 122.5, 122.6 (br), 125.1, 126.8, 128.5, 130.0, 148.1, 150.1, 159.8, 168.6; IR (KBr) 3318, 2981, 2904, 2806, 1752, 1735, 1595, 1510, 1497, 1279, 1215, 1158, 1094 cm^{-1}; MS (70 eV) *m*/*z* 494.2 ([M$^+$], 18), 251.2 (100); EI-HRMS calcd for [M$^+$] $C_{25}H_{26}N_4O_5S$ 494.1624, found 494.1615.

2-(4-(*N*-(2-(5(6)-Cyano-1*H*-benzimidazol-2-yl)-4-methoxyphenyl)sulfamoyl)phenoxy)acetic Acid Ethyl Ester (4h). Starting from 72 mg of aldehyde **9f** (0.183mmol) and 3,4-diaminobenzonitrile (26 mg, 0.20 mmol), benzimidazole **4h** was obtained in 53% yield (FC, EtOAc/hexanes, gradient 1:3 to 1:1). Mp 72−74 °C; ^{1}H NMR (CD_3OD, 400 MHz) δ 1.23 (t, J = 7.1 Hz, 3H), 3.85 (s, 3H), 4.19 (q, J = 7.1 Hz, 2H), 4.57 (s, 2H), 6.57 (d, J = 9.0 Hz, 2H), 7.07 (dd, J = 9.0, 2.9 Hz, 1H), 7.29−7.34 (m, 3H), 7.60 (dd, J = 8.3, 1.5 Hz, 1H), 7.65 (d, J = 9.0 Hz, 1H), 7.72 (br, 1H), 8.06 (br, 1H); ^{13}C NMR (acetone-d_6, 400 MHz) mixture of two tautomers (ratio 2:3) δ 14.4, 56.0, 61.6, 65.5, 106.5, 107.0, 112.6, 113.4, 114.9, 116.8, 118.2, 118.5, 119.3, 119.9, 120.6, 124.3, 124.8, 126.7, 127.5, 129.5, 129.6, 131.5, 131.6, 132.1, 132.2, 133.8, 137.0, 142.6, 145.8, 153.4, 154.1, 157.2, 161.7, 168.3; IR (KBr) 3283, 2936, 2223, 1752, 1735, 1594, 1503, 1318, 1293, 1214, 1159, 1094, 832 cm^{-1}; MS (70 eV) *m*/*z* 506.1 ([M$^+$], 47), 263.1 (100); EI-HRMS calcd for [M$^+$] $C_{25}H_{22}N_4O_6S$ 506.1260, found 506.1251.

2-(4-(*N*-(2-(5(6)-Cyano-1*H*-benzimidazol-2-yl)phenyl)sulfamoyl)-phenoxy)acetic Acid Ethyl Ester (4i). Starting from 150 mg of aldehyde **9i** (0.41 mmol) and 3,4-diaminobenzonitrile (60 mg, 0.41 mmol), benzimidazole **4i** was obtained in 50% yield (FC, EtOAc/hexanes, gradient 1:2 to 1:1). Mp 169−171 °C; ^{1}H NMR (CD_3-OD, 400 MHz) δ 1.21 (t, J = 7.1 Hz, 3H), 4.17 (q, J = 7.1 Hz, 2H), 4.61 (s, 2H), 6.72 (d, J = 9.0 Hz, 2H), 7.22 (ddd, J = 8.5, 7.5, 1.1 Hz, 1H), 7.44 (ddd, J = 8.5, 7.5, 1.5 Hz, 1H), 7.54 (d, J = 9.0 Hz, 2H), 7.58 (dd, J = 8.4, 1.5 Hz, 1H), 7.73 (br, 1H), 7.75 (dd, J = 8.3, 1.0 Hz, 1H), 7.82 (d, J = 7.9, 1.4 Hz, 1H), 8.02 (br, 1H); ^{13}C NMR (CD_3OD, 100 MHz) δ 14.1, 61.1, 64.9, 105.1 (br), 113.2 (br), 115.7, 119.5, 119.9, 124.0, 127.0 (br), 128.2, 129.2, 131.2, 132.0, 136.7 (br), 137.5, 141.4 (br), 144.5 (br), 153.4 (br), 161.2, 168.2; IR (KBr) 3332, 2985, 2220, 1758, 1740, 1594, 1496, 1315, 1154, 1095, 921, 572 cm^{-1}; MS (70 eV) *m*/*z* 476.2 ([M$^+$], 36), 412.1 (32), 325.1 (34), 233.1 (100); EI-HRMS calcd for [M$^+$] $C_{24}H_{20}N_4O_5S$ 476.1154, found 476.1135.

2-(4-(*N*-(2-(5(6)-Methoxy-1*H*-benzimidazol-2-yl)phenyl)sulfamoyl)phenoxy)acetic Acid Ethyl Ester (4k). Starting from 200 mg of aldehyde **9i** (0.55 mmol) and 1,2-diamino-4-methoxybenzene (80 mg, 0.58 mmol), benzimidazole **4k** was obtained in 60% yield (FC, EtOAc/hexanes, gradient 1:3 to 1:1). Mp 72−74 °C; ^{1}H NMR (CD_3OD, 400 MHz) δ 1.19 (t, J = 7.1 Hz, 3H), 3.85 (s, 3H), 4.16 (q, J = 7.1 Hz, 2H), 4.58 (s, 2H), 6.69 (d, J = 9.0 Hz, 2H), 6.91 (dd, J = 8.8, 2.4 Hz, 1H), 7.09 (d, J = 2.2 Hz, 1H), 7.16 (ddd, J = 8.5, 7.8, 1.2 Hz, 1H), 7.33 (ddd, J = 8.3, 7.4, 1.5 Hz, 1H), 7.49−7.54 (m, 3H), 7.69−7.75 (m, 2H); ^{13}C NMR ($CDCl_3$, 100 MHz) δ 14.0, 55.6, 61.8, 64.7, 113.0 (br), 114.1, 116.1, 118.2, 121.5, 124.1, 126.2, 128.9, 130.2, 131.2, 136.8, 149.4 (br), 156.8 (br), 160.6, 168.4; IR (KBr) 3325, 2938, 1752, 1497, 1333, 1283, 1200, 1160, 1148, 1094, 570 cm^{-1}; MS (70 eV) *m*/*z* 481.2 ([M$^+$], 38), 238 (100); EI-HRMS calcd for [M$^+$] $C_{24}H_{23}N_3O_6S$ 481.13076, found 481.13063.

2-(4-(*N*-(6-(1*H*-Benzimidazol-2-yl)benzo[1,3]dioxol-5-yl)sulfamoyl)phenoxy)acetic Acid Ethyl Ester (4l). Starting from 51 mg of aldehyde **9l** (0.12 mmol) and 1,2-phenylenediamine (14 mg, 0.12 mmol), benzimidazole **4l** was obtained in 44% yield (FC, EtOAc/hexanes, gradient 1:3 to 1:1). Mp 168−170 °C; ^{1}H NMR (acetone-d_6, 400 MHz) δ 1.17 (t, J = 7.1, 3H), 4.15 (q, J = 7.1 Hz, 2H), 4.70 (s, 2H), 6.09 (s, 2H), 6.80 (d, J = 8.6 Hz, 2H), 7.28−7.31 (m, 2H), 7.32 (s, 1H), 7.40 (s, 1H), 7.50 (br, 1H), 7.60 (d, J = 8.6 Hz, 2H), 7.76 (br, 1H), 11.78 (br, 1H); ^{13}C NMR (acetone-d_6, 100 MHz) δ 14.4, 61.7, 65.7, 102.8, 103.2, 106.6, 111.2, 112.0, 115.4, 119.4, 123.4, 124.3, 129.9, 132.0, 132.8, 134.7, 143.1, 145.4, 150.5, 151.6, 162.1, 168.7; IR (KBr) 3372, 2922, 1731, 1597, 1499, 1482, 1429, 1328, 1279, 1250, 1161, 1098, 1037, 916, 769 cm^{-1}; MS (70 eV) *m*/*z* 495 ([M$^+$], 32), 252 (100); EI-HRMS calcd for [M$^+$] $C_{24}H_{21}N_3O_7S$ 495.1100, found 495.1089.

General Procedure B: Hydrolysis of Esters 4 to Acids 5. A solution of the corresponding ester (0.085 mmol) and LiOH·H_2O (87 mg) in 1.5 mL of MeOH/water/THF (1:1:2) was heated at reflux for 3 h. After removing the organic solvents under reduced pressure, the residue was acidified with aqueous HCl (1 M) until the acid precipitated. The product was filtered off, washed with water, and dried in vacuum to give the free acid.

2-(4-(*N*-(2-(1*H*-Benzimidazol-2-yl)-5-cyanophenyl)sulfamoyl)-phenoxy)acetic Acid (5b). From **4b**, 92% yield. Mp >210 °C (dec); ^{1}H NMR (CD_3OD, 400 MHz) δ 4.60 (s, 2H), 6.80 (d, J = 8.9 Hz, 2H), 7.33−7.38 (m, 2H), 7.51 (dd, J = 8.2 Hz, 1.3 Hz, 1H), 7.62 (d, J = 8.9 Hz, 2H), 7.65−7.69 (m, 2H), 7.97 (d, J = 8.2 Hz, 1H), 8.00 (d, J = 1.4 Hz, 1H); ^{13}C NMR (DMSO-d_6, 100 MHz) δ 65.7, 111.7, 114.5, 115.1, 118.7, 121.0, 121.5, 122.6, 128.1, 128.5, 131.3, 133.6, 137.5, 143.0, 150.2, 160.4, 170.2; IR (KBr) 3071, 2922, 2851, 2233, 1735, 1594, 1581, 1570, 1497, 1401, 1333, 1274, 1155, 1094, 566, 552 cm^{-1}; ESI-MS *m*/*z* 449.0918 ([M + H]$^+$); ESI-HRMS calcd for [M + H]$^+$ $C_{22}H_{17}N_4O_5S$ 449.0914, found 449.0913.

2-(4-(*N*-(5(6)-Cyano-2-(5-methoxy-1*H*-benzoimidazol-2-yl)-phenyl)sulfamoyl)phenoxy)acetic Acid (5c). From **4c**, 85% yield. Mp 112−115 °C; ^{1}H NMR (CD_3OD, 400 MHz) δ 3.89 (s, 3H), 4.61 (s, 2H), 6.82 (d, J = 9.0 Hz, 2H), 6.98 (dd, J = 8.9 Hz, 2.4 Hz, 1H), 7.12 (d, J = 2.4 Hz, 1H), 7.51 (dd, J = 8.2 Hz, 1.6 Hz, 1H), 7.58 (d, J = 9.1, 1H), 7.62 (d, J = 9.0 Hz, 2H), 7.92 (d, J = 8.2 Hz, 1H), 8.00 (d, J = 1.3 Hz, 1H); ^{13}C NMR (DMSO-d_6, 100 MHz) δ 55.6, 64.9, 96.7, 111.8, 113.6, 114.9, 118.1, 120.1, 121.2, 126.0, 128.0, 128.6, 130.8, 137.9, 148.1, 156.6, 161.1, 169.3; IR (KBr) 2924, 2851, 2231, 1735, 1636, 1594, 1570, 1496, 1405, 1272, 1157, 1094, 833, 554 cm^{-1}; MS (70 eV) *m*/*z* 478 ([M$^+$], 8), 263.1 (100); EI-HRMS calcd for [M$^+$] $C_{23}H_{18}N_4O_6S$ 478.0947, found 478.0946.

(4-(2-(1*H*-Benzimidazol-2-yl)-5-thiazol-2-yl-phenylsulfamoyl)-phenoxy)-acetic Acid (5d). From **4d**, 71% yield. Mp >300 °C; ^{1}H NMR (CD_3OD, 400 MHz) δ 4.43 (s, 2H), 6.73 (d, J = 9.0 Hz, 2H), 7.30−7.36 (m, 2H), 7.58 (d, J = 9.0 Hz, 2H), 7.64−7.71 (m, 3H), 7.78 (dd, J = 8.1, 1.8 Hz, 1H), 7.89−7.95 (m, 2H), 8.33 (d, J = 1.7 Hz, 1H); ^{13}C NMR (DMSO-d_6, 100 MHz) δ 66.0, 114.9, 115.9, 117.5, 121.5, 123.1, 128.6, 130.9, 134.4, 139.0, 144.3, 150.2, 161.7, 166.0, 169.6; IR (KBr) 3401 (br), 1612, 1595, 1577, 1496, 1426, 1324, 1247, 1162, 1095, 1065, 576 cm^{-1}; FAB-MS (thioglycerol) *m*/*z* 507 ([M$^+$], 24), 349.1 (26), 327 (28), 311 (62), 279 (58), 237 (100); FAB-HRMS calcd for [M$^+$] $C_{24}H_{19}N_4O_5S_2$ 507.0797, found 507.0835.

(4-[2-(1*H*-Benzimidazol-2-yl)-5-methoxy-phenylsulfamoyl]-phenoxy)-acetic Acid (5e). From **4e**, 88% yield. Mp 128−131 °C; ^{1}H NMR (CD_3OD, 400 MHz) δ 3.72 (s, 3H), 4.52 (s, 2H), 6.67 (dd, J = 8.8, 2.5 Hz, 1H), 6.73 (d, J = 8.9 Hz, 2H), 7.09 (d, J = 2.5 Hz, 1H), 7.22−7.26 (m, 2H), 7.54−7.58 (m, 4H), 7.67 (d, J = 8.8 Hz, 1H); ^{13}C NMR (CD_3OD, 100 MHz) δ 56.0, 65.9, 107.8, 111.3, 111.8, 115.35, 115.42, 124.1, 129.8, 130.0, 132.2, 137.9, 139.8, 151.5, 162.5, 162.6, 171.9; IR (KBr) 2934, 1735, 1629, 1611, 1594, 1581, 1497, 1302, 1261, 1230, 1155, 1092 cm^{-1}; MS (70 eV) *m*/*z* 454 ([M + H$^+$] 100); ESI-TOF-HRMS calcd for [M + H$^+$] $C_{22}H_{20}N_3O_6S$ 454.1067, found 454.1097.

2-(4-(*N*-(2-(1*H*-Benzimidazol-2-yl)-4-methoxyphenyl)sulfamoyl)-phenoxy)acetic Acid (5f). From **4f**, 96% yield. Mp 187−190 °C; ^{1}H NMR (DMSO-d_6, 400 MHz) δ 3.81 (s, 3H), 4.64 (s, 2H), 6.82 (d, J = 8.9 Hz, 2H), 7.06 (dd, J = 9.0, 2.8 Hz, 1H), 7.29−7.34 (m, 2H), 7.54 (d, J = 8.9 Hz, 2H), 7.59 (d, J = 8.9 Hz, 1H), 7.59 (d, J = 2.9 Hz, 1H), 7.68 (br, 2H); ^{13}C NMR (DMSO-d_6, 100 MHz) δ 55.6, 64.5, 109.4, 111.9, 114.5, 114.6, 116.8, 117.6, 121.4, 123.3 (br), 128.5, 130.0, 130.6, 149.9, 155.2, 160.6, 169.1; IR (KBr) 3067, 2928, 2853, 2736, 1735, 1594, 1582, 1500, 1330, 1233, 1159, 1095,

835 cm^{-1}; MS (70 eV) *m*/*z* 453 ([M$^+$], 18), 238 (100); EI-HRMS calcd for [M$^+$] $C_{22}H_{19}N_3O_6S$453.0994, found 453.1009.

2-(4-(*N*-(2-(1*H*-Benzimidazol-2-yl)-4-(dimethylamino)phenyl)-sulfamoyl)phenoxy)acetic Acid (5g). From **4g**, 67% yield. Mp >230 °C; ^{1}H NMR (CD_3OD, 400 MHz) δ 2.93 (s, 6H), 4.28 (s, 2H), 6.58 (d, J = 9.3 Hz, 2H), 6.81 (d, J = 7.7 Hz, 1H), 7.23−7.32 (m, 5H), 7.43 (d, J = 8.8 Hz, 1H), 7.59−7.63 (m, 2H); ^{13}C NMR (DMSO-d_6, 100 MHz) δ 41.4, 67.6, 112.0, 113.8, 116.7, 118.2, 120.5, 121.0, 127.6, 128.6, 143.1, 153.8, 159.7, 171.0; IR (KBr) 3436, 1686, 1648, 1444, 1384, 1212, 1140, 846, 804, 726 cm^{-1}; MS (70 eV) *m*/*z* 466.1 ([M$^+$], 9), 252.2 (100), 238.1 (100), 184 (44), 125 (46); EI-HRMS calcd for [M$^+$] $C_{23}H_{22}N_4O_5S$ 466.1311, found 466.1326.

2-(4-(*N*-(2-(5(6)-Cyano-1*H*-benzimidazol-2-yl)-4-methoxyphenyl)sulfamoyl)phenoxy)acetic Acid (5h). From **4h**, 49% yield. Mp 236−239 °C; ^{1}H NMR (DMSO-d_6, 400 MHz) δ 3.85 (s, 3H), 4.54 (s, 2H), 6.57 (d, J = 9.0 Hz, 2H), 7.08 (dd, J = 9.0, 2.9 Hz, 1H), 7.30 (d, J = 9.0 Hz, 2H), 7.32 (d, J = 2.9 Hz, 1H), 7.61 (dd, J = 8.4, 1.5 Hz, 1H), 7.65 (d, J = 9.0 Hz, 1H), 7.73 (br, 1H), 8.05 (br, 1H); ^{13}C NMR (DMSO-d_6, 100 MHz) δ 55.6, 64.6, 104.8, 112.4, 114.4, 117.6, 119.5, 122.5, 126.3, 128.5, 130.0, 130.2, 152.8, 155.5, 160.7, 169.1; IR (KBr) 3293 (br), 3078, 2927, 2224, 1735, 1592, 1502, 1339, 1240, 1158, 1095, 835, 570 cm^{-1}; ESI-MS *m*/*z* 479.10 ([M + H$^+$]); ESI-HRMS calcd for [M + H$^+$] $C_{23}H_{19}N_4O_6S$ 479.1020, found 479.1053.

2-(4-(*N*-(2-(5(6)-Cyano-1*H*-benzimidazol-2-yl)phenyl)sulfamoyl)-phenoxy)acetic Acid (5i). From **4i**, 68% yield. Mp 279−281 °C; ^{1}H NMR (DMSO-d_6, 400 MHz) δ 4.69 (s, 2H), 6.92 (d, J = 8.9 Hz, 2H), 7.26 (td, J = 7.4, 1.0 Hz, 1H), 7.50 (td, J = 7.4, 1.4 Hz, 1H), 7.63−7.62 (m, 4H), 7.81 (br, 1H), 8.05 (d, J = 7.8 Hz, 1H), 8.24 (br, 1H), 12.71 (br, 1H); ^{13}C NMR (DMSO-d_6, 100 MHz) δ 64.6, 104.8, 114.8, 115.3, 119.0, 119.5, 123.5, 126.3, 126.4, 127.9, 128.8, 130.5, 131.6, 137.1, 153.0, 161.0, 169.2; IR (KBr) 3300, 2923, 2220, 1741, 1594, 1581, 1492, 1339, 1251, 1160, 1095, 576 cm^{-1}; MS (70 eV) *m*/*z* 448 ([M$^+$], 10), 234.1 (100); EI-HRMS calcd for [M$^+$] $C_{22}H_{16}N_4O_5S$ 448.0841, found 448.0867.

2-(4-(*N*-(2-(5(6)-Methoxy-1*H*-benzimidazol-2-yl)phenyl)sulfamoyl)phenoxy)acetic Acid (5k). From **4k**, 90% yield. Mp 133−135 °C; ^{1}H NMR (CD_3OD, 400 MHz) δ 3.83 (s, 3H), 4.53 (s, 2H), 6.68 (d, J = 9.0 Hz, 2H), 6.91 (dd, J = 8.8, 2.4 Hz, 1H), 7.08 (d, J = 2.3, 1H), 7.17 (td, J = 7.6, 1.2 Hz, 1H), 7.33 (td, J = 7.5, 1.5 Hz, 1H), 7.46−7.51 (m, 3H), 7.61 (dd, J = 9.2, 1.0 Hz, 1H), 7.71 (dd, J = 7.9, 1.4 Hz, 1H); ^{13}C NMR (CD_3OD, 100 MHz) δ 56.2, 65.9, 97.5, 114.2, 115.3, 116.9, 119.9, 123.1, 125.6, 128.1, 130.0, 131.3, 132.2, 133.6, 137.8, 138.3, 150.6, 158.3, 162.4, 171.8; IR (KBr) 3068, 2943, 1636, 1595, 1492, 1403, 1332, 1302, 1274, 1233, 1155, 824, 573 cm^{-1}; MS (70 eV) *m*/*z* 453.2 ([M$^+$], 26), 238 (100); EI-HRMS calcd for [M$^+$] $C_{22}H_{19}N_3O_6S$ 453.0995, found 453.1032.

2-(4-(*N*-(6-(1*H*-Benzimidazol-2-yl)benzo[1,3]dioxol-5-yl)sulfamoyl)phenoxy)acetic Acid (5l). From **4l**, 81% yield. Mp >128 °C (dec); ^{1}H NMR (CD_3OD, 400 MHz) δ 4.34 (s, 2H), 6.00 (s, 2H), 6.57 (d, J = 9.0 Hz, 2H), 7.18 (s, 1H), 7.22 (s, 1H), 7.23−7.28 (m, 2H), 7.35 (d, J = 9.0 Hz, 2H), 7.55−7.58 (m, 2H); ^{13}C NMR (DMSO-d_6, 100 MHz) δ 67.0, 101.6, 102.6, 106.6, 110.6, 114.9, 115.0, 123.2, 128.8, 130.0, 133.5, 144.3, 149.5, 151.0, 162.3, 171.1; IR (KBr) 3068, 2923, 1595, 1503, 1484, 1256, 1226, 1157, 1037 cm^{-1}; MS (70 eV) 467 ([M$^+$], 18), 252.1 (100); EI-HRMS *m*/*z* calcd for [M$^+$] $C_{22}H_{17}N_3O_7S$ 467.0787, found 467.0791.

4-(2-Formyl-4-methoxy-phenylsulfamoyl)-phenoxy]-acetic Acid Ethyl Ester (9f). A solution of 5-methoxy-2-nitrobenzaldehyde[38] **1f** (250 mg, 1.38 mmol) in methanol (15 mL) was hydrogenated at atmospheric pressure in the presence of Pd on activated carbon (10 wt %, 50 mg) as catalyst. After completion of the reaction (3 h) the reaction mixture was filtered through a pad of Celite and concentrated under reduced pressure. The crude amine **6f** was immediately dissolved in anhydrous pyridine (4 mL), and ethyl (4-chlorosulfonyl-phenoxy)-acetate[14] **10** (770 mg, 2.76 mmol) was added. The mixture was stirred at room temperature for 3 h, diluted with water (10 mL), and extracted twice with ethyl acetate (20 mL). The combined organic extracts were dried with $MgSO_4$ and concentrated under reduced pressure. The residue was purified on silica gel (FC, gradient hexanes/EtOAc, 2:1 to 1:1) providing 243 mg of aldehyde **9f** as a tan solid (0.62 mmol, 45%). Mp 133−135 °C; ^{1}H NMR ($CDCl_3$, 400 MHz) δ 1.28 (t, J = 7.1 Hz, 3H), 3.81 (s, 3H), 4.25 (q, J = 7.1 Hz, 2H), 4.62 (s, 2H), 6.87 (d, J = 8.9 Hz, 2H), 7.05 (d, J = 3.0 Hz, 1H), 7.09 (dd, J = 9.0, 3.3 Hz, 1H), 7.67 (d, J = 9.0 Hz, 1H), 7.73 (d, J = 8.9, 2H), 9.73 (s, 1H), 10.19 (s, 1H); ^{13}C NMR ($CDCl_3$, 100 MHz) δ 14.2, 55.7, 61.7, 65.2, 114.6, 119.2, 121.0, 121.9, 123.4, 129.2, 131.7, 132.6, 155.5, 160.9, 167.6, 194.3; IR (KBr) 2924, 1735, 1654, 1593, 1580, 1497, 1271, 1163, 1149, 1095 cm^{-1}; MS (70 eV) *m*/*z* 393 ([M$^+$], 5), 241 (11), 129 (100); EI-HRMS calcd for [M$^+$] $C_{18}H_{19}NO_7S$ 393.0882, found 393.0869.

2-(4-(*N*-(4-(Dimethylamino)-2-formylphenyl)sulfamoyl)phenoxy)acetic Acid Ethyl Ester (9g). A solution of 2-nitro-5-dimethylamino-benzaldehyde **1g** (255 mg, 1.3 mmol) in methanol (50 mL) was hydrogenated at room temperature and ambient pressure in the presence of Pd on activated carbon as catalyst (60 mg, 5 wt % Pd). After completion of the reaction (TLC), the catalyst was filtered off through a pad of Celite, and the solvent was evaporated under reduced pressure. The crude amine (227 mg) was immediately dissolved in pyridine (3 mL), and (4-chlorosulfonyl-phenoxy)-acetic acid ethyl ester[14] **10** (462 mg, 1.66 mmol) was added. After stirring for 2 h at room temperature, the reaction mixture was poured into 1 M aqueous HCl (10 mL), and the product was extracted twice with ethyl acetate. The combined organic extracts were dried with $MgSO_4$, filtered, and concentrated under reduced pressure. The crude product was recrystallized from diethyl ether to give 146 mg (0.36 mmol) of aldehyde **9g** as a tan solid (28% total yield). Mp 85−87 °C; ^{1}H NMR ($CDCl_3$, 400 MHz) δ 1.27 (t, J = 7.1 Hz, 3H), 2.94 (s, 6H), 4.25 (q, J = 7.1 Hz, 2H), 4.61 (s, 2H), 6.80 (d, J = 3.3 Hz, 1H), 6.84 (d, J = 9.3 Hz, 2H), 6.88 (dd, J = 8.8, 3.3 Hz, 1H), 7.57 (d, J = 8.8 Hz, 1H), 7.67 (d, J = 8.8 Hz, 2H), 9.70 (s, 1H), 9.85 (s, 1H); ^{13}C NMR ($CDCl_3$, 100 MHz) δ 14.1, 40.5, 61.6, 65.1, 114.4, 118.1, 119.0, 121.7, 124.1, 128.1, 129.1, 131.8, 147.1, 160.7, 167.6, 195.1; IR (KBr) 3206, 2987, 2812, 1762, 1663, 1591, 1507, 1364, 1204, 1152, 1094, 921, 563 cm^{-1}; MS (70 eV) *m*/*z* 406.2 ([M$^+$], 68), 163.1 (100), 135.1 (100); EI-HRMS calcd for [M$^+$] $C_{19}H_{22}N_2O_6S$ 406.1199, found 406.1197.

2-(4-(*N*-(6-Formylbenzo[1,3]dioxol-5-yl)sulfamoyl)phenoxy)-acetic Acid Ethyl Ester (9l). A solution of 6-nitropiperonal (1.0 g, 5.12 mmol) in ethanol (30 mL) was hydrogenated at room temperature and ambient pressure in the presence of Pd on activated carbon (200 mg, 5% Pd) as catalyst. After completion of the reaction (2 h), the catalyst was filtered through a pad of Celite, and the filtrate was concentrated under reduced pressure providing 885 mg of crude **7l** as a yellow solid. A solution of crude amine **7l** (885 mg) and (4-chlorosulfonyl-phenoxy)acetic acid ethyl ester[14] **10** (1.79 g, 6.4 mmol) in 22 mL of pyridine was stirred at room temperature for 48 h. The mixture was poured into 1 N HCl and extracted twice with ethyl acetate. The combined organic extracts were dried with anhydrous $MgSO_4$, filtered, and concentrated under reduced pressure. The crude product was purified by silica FC (EtOAc/hexanes, gradient 1:2 to 1:1) to give 584 mg of intermediate **8l** as a yellowish solid. A mixture of intermediate **8l** (576 mg, 1.41 mmol) and MnO_2 (1.6 g, 18.4 mmol) in 5 mL of CH_2Cl_2 was stirred overnight at room temperature. The reaction mixture was filtered through a pad of Celite and concentrated under reduced pressure to give aldehyde **9l** as a pale yellow solid (378 mg, 0.928 mmol, 18% yield over three steps). Mp 166−168 °C; ^{1}H NMR ($CDCl_3$, 400 MHz) δ 1.28 (t, J = 7.1 Hz, 3H), 4.26 (q, J = 7.1 Hz, 2H), 4.64 (s, 2H), 6.04 (s, 2H), 6.90 (d, J = 9.0 Hz, 2H), 6.91 (s, 1H), 7.27 (s, 1H), 7.79 (d, J = 9.0 Hz, 2H), 9.57 (s, 1H), 11.07 (s, 1H); ^{13}C NMR ($CDCl_3$, 100 MHz) δ 14.3, 61.8, 65.2, 99.6, 102.5, 112.8, 114.8, 115.9, 129.3, 131.8, 137.9, 143.5, 153.7, 161.1, 167.7, 192.2; IR (KBr) 2913, 1735, 1641, 1594, 1487, 1361, 1283, 1245, 1225, 1151, 1093,

1038, 574 cm^{-1}; MS (70 eV) 407 ([M^+], 37), 164 (100); EI-HRMS *m*/*z* calcd for [M^+] $C_{18}H_{17}NO_8S$ 407.0675, found 407.0662.

Steady-State Absorption and Fluorescence Spectroscopy. All sample solutions were filtered through 0.45 μm Teflon membrane filters to remove interfering dust particles or fibers. UV−vis absorption spectra were recorded at 25 °C using a UV−vis spectrometer with a constant-temperature accessory. Steady-state emission and excitation spectra were recorded with a fluorimeter and FELIX software. For all measurements the path length was 1 cm with a cell volume of 3.0 mL. The fluorescence spectra have been corrected for the spectral response of the detection system (emission correction file provided by the instrument manufacturer) and for the spectral irradiance of the excitation channel (via calibrated photodiode). Quantum yields were determined using quinine sulfate dihydrate in 0.5 M H_2SO_4 as fluorescence standard ($\Phi_F = 0.54 \pm 0.05$).[42]

Determination of pK_a Values. A combination microelectrode electrode was calibrated for $-\log[H_3O^+]$ by titration of a standardized HCl solution (0.1 N volumetric standard) with KOH (0.1 N volumetric standard) at 25 °C and 0.1 M ionic strength (KCl). The end point, electrode potential, and slope were determined by Gran's method[43] as implemented in the software GLEE.[44] The calibration procedure was repeated three times prior to each pK_a value determination. The electrode potentials were measured with a pH/ion analyzer, and the potentials were reproducible with ±0.1 mV accuracy. A series of UV−vis spectra of each fluorophore were acquired for which $-\log[H_3O^+]$ was varied between 3 and 10. The emf of each solution was directly measured in the quartz cell and converted to $-\log[H_3O^+]$ using $E°$ and slope as obtained from the electrode calibration procedure. The raw spectral and emf data were then processed via nonlinear least-squares fit analysis using the SPECFIT software package,[45] providing deconvoluted spectra for each species present as well as the corresponding acidity constants for all involved protonation equilibria.

Acknowledgment. We thank Dr. Leslie Gelbaum for acquisition of the 2D NMR data and David Bostwick for mass spectral characterization of all compounds. This work was supported by the National Institutes of Health (DK68096) and the Georgia Institute of Technology.

Supporting Information Available: ^1H and ^{13}C NMR spectra for compounds **1b**, **1d**, **1e**−**1g**, **2b**−**2e**, **3b**−**3e**, **4b**−**4l**, **5b**−**5l**, **9f**, **9g**, **9l**. This material is available free of charge via the Internet at http://pubs.acs.org.

JO070433L

(42) Demas, J. N.; Crosby, G. A. *J. Phys. Chem.* **1971**, *75*, 991−1024.
(43) Gran, G. *Analyst* **1951**, *77*, 661.
(44) Gans, P.; O'Sullivan, B. *Talanta* **2000**, *51*, 33−37.
(45) Binstead, R. A.; Zuberbühler, A. D. *SPECFIT*, v. 3.0.27; Spectrum Software Associates: Marlborough, MA, 2001.